COMPARISON OF A NOVEL STANDARDIZED UPTAKE VALUE (SUV) CALCULATION SCHEME USING MATLAB TO XELERIS® WORKSTATION

PAWITRA MASA-AH

A THESIS SUBMITTED IN PARTIAL FULFILLMENT
OF THE REQUIREMENTS FOR THE DEGREE OF
MASTER OF SCIENCE (RADIOLOGICAL SCIENCE)
FACULTY OF GRADUATE STUDIES
MAHIDOL UNIVERSITY
2011

Thesis
entitled

COMPARISON OF A NOVEL STANDARDIZED UPTAKE VALUE (SUV) CALCULATION SCHEME USING MATLAB TO XELERIS® WORKSTATION

Pawitra Masa-ah.

Miss Pawitra Masa-ah
Candidate

S. Soongsathitanon.

Lect. Somphob Soongsathitanon, Ph.D.
Major advisor

M. Tuntawiroon

Assoc.Prof. Malulee Tuntawiroon, M.S.
Co-advisor

B. Mahaisaviraya

Prof. Banchong Mahaisaviraya,
M.D., Dip Thai Board of Orthopedics
Dean
Faculty of Graduate Studies
Mahidol University

N. Sritongkul

Assoc.Prof. Nopamon Sritongkul, M.S.
Program Director
Master of Science Program in
Radiological Science, Faculty of
Medicine Siriraj Hospital
Mahidol University

Thesis
entitled

COMPARISON OF A NOVEL STANDARDIZED UPTAKE VALUE (SUV) CALCULATION SCHEME USING MATLAB TO XELERIS® WORKSTATION

was submitted to the Faculty of Graduate Studies, Mahidol University
for the Degree of Master of Science (Radiological Science)
on
March 10, 2011

Pawitra Masa-ah.
.....
Miss Pawitra Masa-ah
Candidate

Supphanat
.....
Mr. Supphanat Kanokphara, Ph.D.
Chair

S. Soongsathitanon
.....
Mr. Somphob Soongsathitanon, Ph.D.
Member

M. Tuntawiroon
.....
Assoc.Prof.Malulee Tuntawiroon, M.S.
Member

B. Mahaisa
.....
Prof. Banchong Mahaisaviraya,
M.D., Dip Thai Board of Orthopedics
Dean
Faculty of Graduate Studies
Mahidol University

T. Kulfean
.....
Clin.Prof.Teerawat Kulthanan, M.D
Dean
Faculty of Medicine Siriraj Hospital
Mahidol University

ACKNOWLEDGEMENTS

The successful completion of this thesis was made possible through the invaluable contribution of a number of people. To say “Thank you” is not even enough to express here.

First of all, I would like to express my deepest sense of gratitude to my advisor, Dr. Somphob Soongsathitanon for his understanding and patient advice throughout my graduate experience and without his encouragement, I would not have the great opportunity to present this thesis at Taipei, Taiwan. It is one of the best experiences in my life!

My sincere thanks go to Assoc.Prof. Malulee Tuntawiroon, my co-advisor, for the continuous guidance, invaluable suggestions and comments about the scope of the study and data analysis. I am very much grateful for the knowledge.

I am also very grateful to all teachers and lecturers of Radiological Science programme, Mahidol University for their selfless efforts to pass on their knowledge to me.

Thanks to all staffs and colleagues at division of nuclear medicine, department of radiology, faculty of medicine Siriraj hospital, for the friendly helps and supports.

To my family, I have no suitable word that can fully describe their everlasting love for me. I am greatly indebted and appreciate very much to my beloved parents and my two lovely sisters. Thanks for always being behind me and pushing me to be the best that I can be.

Pawitra Masa-ah

COMPARISON OF A NOVEL STANDARDIZED UPTAKE VALUE (SUV) CALCULATION SCHEME USING MATLAB TO XELERIS® WORKSTATION

PAWITRA MASA-AH 4937092 SIRS/M

M.S. (RADIOLOGICAL SCIENCE)

THESIS ADVISORY COMMITTEE: SOMPHOB SOONGSATHITANON, Ph.D., MALULEE TUNTAWIROON, M.S.

ABSTRACT

Positron emission tomography - computed tomography (PET/CT) is currently an important cancer imaging tool, both for diagnosis and staging. The standardized uptake value (SUV) is used for quantitative analysis of dynamic data and represents the ratio of ^{18}F-FDG uptake within a region of interest (ROI) relative to its background. A malignant lesion is considered to have a high uptake based on the uptake of the ^{18}F-FDG radiopharmaceutical. In this research, the scheme of SUV calculation was created by using MATLAB. The sample source of this research is DICOM files. SUV was calculated from the PET images and related data such as patient weight, activity dose, rescale slope and rescale intercept. This data was taken from the DICOM files. The DICOM format is a universal and unique file type containing parts of images and metadata (headers). The performance of the MATLAB scheme was tested by comparing the obtained SUV_{max} to that obtained from the well-known application software (Xeleris Workstation).

108 slices of DICOM files were obtained from 11 patients (8 men, 3 women) and comparative analysis of both systems was done by drawing the region of interest (ROI) in a slice with the same size and position. The results showed that the correlation between the two systems is statistically significant with a 99% confidence interval. The average percentage of accuracy is 85% for the report at a 95% confidence interval. The result showed a percentage of accuracy in the range of 83.91% to 86.48% at a 95% confidence interval. The performance test of the new scheme demonstrated agreeable results that are practical to medical prognosis and research.

The results showed that the SUV from the scheme created by MATLAB could be used interchangeably with a PET/CT Xeleris® workstation. There are many benefits of adopting a PET/CT analysis tool within a medical imaging system. The interchangeability of this scheme offers user convenience and approachability of data and is a stand-alone application that allows more accessibility. Physicians can interpret PET/CT scans without further applications of other software.

KEY WORDS: PET-CT/ SUV / DICOM

90 pages

เปรียบเทียบเทคนิคการคำนวณค่า Standardized Uptake Value (SUV) ที่สร้างขึ้นโดย MATLAB กับ Xeleris® workstation.

COMPARISON OF A NOVEL STANDARDIZED UPTAKE VALUE (SUV) CALCULATION SCHEME USING MATLAB TO XELERIS® WORKSTATION

ปวิตรา หมะสะอะ 4937092 SIRS/M

วท.ม. (วิทยาศาสตร์รังสี)

คณะกรรมการที่ปรึกษาวิทยานิพนธ์: สมภพ สูงสถิตานนท์, Ph.D.(Image Processing), มลุลี ตัณฑวิรุฬห์, M.S. (Nuclear Medicine)

บทคัดย่อ

PET/CT เป็นเครื่องมือที่ใช้ถ่ายภาพในงานเวชศาสตร์นิวเคลียร์ เพื่อการตรวจวินิจฉัยและติดตามผลการรักษาโรคมะเร็ง โดยจะพบการจับสารเภสัชรังสี ^{18}F-FDG ที่บริเวณรอยโรค นอกจากภาพรังสี แพทย์ใช้ค่า Standardized Uptake Value (SUV) ร่วมในการประเมินผลการวินิจฉัย ค่า SUV ก็เป็นข้อมูลเชิงปริมาณ แสดงสัดส่วนการ uptake F18-FDG บริเวณที่สนใจ เทียบกับ Background การแสดงค่า SUV จะต้องอาศัยซอฟแวร์ ซึ่งมักจะติดตั้งอยู่ใกล้เครื่องตรวจหรืออยู่ในบริเวณที่ PACS ครอบคลุม อีกทั้งซอฟแวร์ดังกล่าวมักจะเป็นผู้ผลิตเดียวกับเครื่องตรวจซึ่งรองรับได้เฉพาะไฟล์ที่ได้จากเครื่องตรวจเดียวกันเท่านั้น จากข้อจำกัดของการวิเคราะห์ข้อมูลดังกล่าว ทำให้เกิดการวิจัยครั้งนี้ โดยนำเสนอ เทคนิคใหม่ในการคำนวณค่า SUV ที่สร้างขึ้นโดย MATLAB เป็นเทคนิคที่ใช้ตัวอย่างไฟล์ภาพรังสีไดคอม (DICOM) แล้วทดสอบประสิทธิภาพ โดยนำค่า SUV ที่ได้ เปรียบเทียบกับค่าที่ได้จาก Xeleris Workstation ซึ่งเป็นซอฟแวร์ที่ทางศูนย์ภาพวินิจฉัยศิริราช ใช้ในการตรวจ PET/CT ในปัจจุบัน การศึกษาเปรียบเทียบจากไฟล์ไดคอม 108 ตัวอย่าง จากผู้ป่วย 11 คน ในการทดสอบแต่ละคู่เทคนิค เป็นการวิเคราะห์บนไฟล์เดียวกันซึ่งรอย ROI (region of interest) มีขนาดและตำแหน่งเดียวกัน จากผลการทดสอบหาค่าความสัมพันธ์ โดยใช้สหสัมพันธ์แบบเพียร์สัน (Pearson's Correlation) พบว่าค่า SUV ที่จากทั้งสองเทคนิคสัมพันธ์กันอย่างมีนัยสำคัญที่ความเชื่อมั่นร้อยละ 99 และค่า SUV จากเทคนิคที่สร้างขึ้นโดย MATLAB มีความถูกต้องเฉลี่ยเท่ากับร้อยละ 85 เทียบกับค่า SUV จาก Xeleris Workstation ผลการศึกษาครั้งนี้แสดงให้เห็นว่าเทคนิคใหม่นี้สามารถพัฒนาให้สามารถใช้เพื่อการวิเคราะห์ SUV ได้เพิ่มความสะดวกยิ่งขึ้นโดยสามารถวิเคราะห์ค่า SUV บนคอมพิวเตอร์ที่ติดตั้ง MATLAB ซึ่งเป็นโปรแกรมพื้นฐานที่นักวิทยาศาสตร์ใช้กันโดยแพร่หลายอยู่แล้ว

90 หน้า

CONTENTS

CONTENTS (cont.)

LIST OF TABLES

LIST OF FIGURES

LIST OF FIGURES (cont.)

LIST OF FIGURES (cont.)

LIST OF ABBREVIATIONS

Abbreviation	Term
PET	Positron emission tomography
CT	X-ray computed tomography
F18-FDG	Fluoride-18-Deoxyglucose or Fluorodeoxyglucose
SUV	Standardized Uptake Values
bw	body weight
bsa	body surface area
ROI	Region of Interest
VOI	Volume of Interest
LOR	Line of Response
FOV	Field of View
MeV	Mega Electron Volt
PMT	Photo Multiplier Tubes
PHA	Pulse Height Analyzer
FBP	Filtered Back-Projection
PACS	Picture Archiving and Communication Systems
DICOM	Digital Imaging and Communications in Medicine
NEMA	the National Electrical Manufacturers Association
ACR	the American College of Radiology
RTP	Radiation treatment planning
mCi	Milli curie
A	Mass Number
Z	Atomic Number
2D	Two Dimensions
3D	Three Dimensions

CHAPTER I
INTRODUCTION

In Nuclear medicine, Positron Emission Tomography (PET) scanner plays an important role in both diagnosis and staging of cancers. The hybrid system of a PET scanner combined with CT scanner (PET/CT) has gained popularity in the oncological community since its commercial introduction to the market in early 2001.

PET/CT is the fusion of the best of both worlds, it was combined by functional data and the structural anatomic information that lets us see the disease in a way that is diagnostically very powerful.

In addition to providing anatomic data, the CT transmission scan can be used to generate an attenuation map that can be used to correct this attenuation effect. This correction process is essential for quantitative assessment (SUV standardized uptake values). The images of PET/CT are normally presented and viewed in 3 planes (coronal, transaxial, and sagittal) as well as a 3D maximum intensity projection (M.I.P.), which can be rotated while viewing. The CT, corrected and uncorrected PET scans, as well as the fusion image can be viewed on a single page. So in this research we used the DICOM file that has been through the attenuation correction in transaxial plane.

PET/CT is classified as medical device that measures radioactive traces injected into the body. The PET tracer (F18-FDG) has two parts: glucose, and a mildly radioactive component. As the tracer moves through the body the cells that are active take up the glucose along with the radioactive part of tracer.

In fact, FDG is not cancer specific and will accumulate in areas with high levels of metabolism and glycolysis. Therefore the increased uptake can be expected in sites of hyperactivity (muscular, nervous), active inflammation (infection, sarcoid, arthritis, etc.), tissue repair, etc.

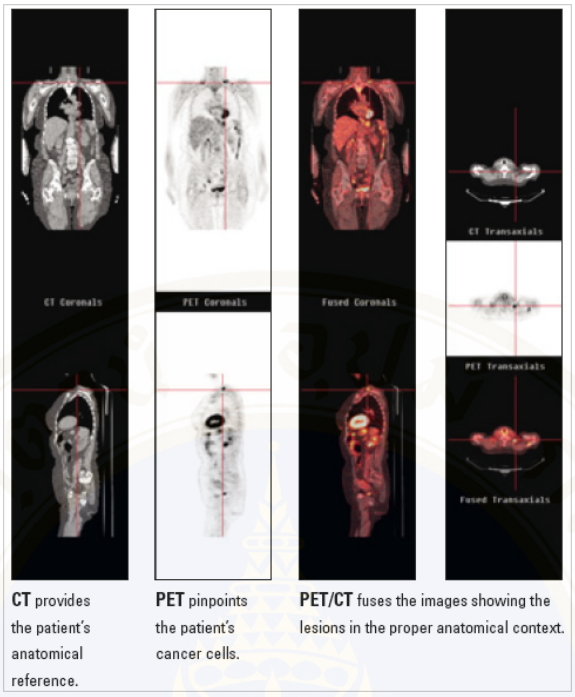

Figure 1.1 The example of all image planes from PET/CT : coronal plane(above), sagittal plane(below), transaxial plane(right) (http://www.westcoastradiology.net/images/pic-pet-ct-1.jpg)

PET shows a metabolism of cell or tissue by displaying the image with the semi-quantitative value called Standardized Uptake Value (SUV). In PET studies some case or some applications the PET image alone may be sufficient for clinical diagnosis such as brain scan for diagnosis Alzheimer's dementia. However Qualitative approaches are often used for practical reason,i.e. in cases that need estimating the concentration of tracer, but not a full kinetic analysis, semi-quantitative is often used.

The simplest semi-quantitative approach is to estimate the concentration of tracer in a given region from PET images by using an ROI analysis. The semi-quantitative measure of local FDG uptake has been developed and utilized in differentiating benign from malignant lesion since malignant lesions in general having greater uptake.

SUV (Standardized Uptake Value) is the value that often used in PET scan. It is most commonly used semi-quantitative parameter utilized for analyzing FDG-PET images in routine clinical practice. It came to be used as a tool to supplement visual interpretation.[1]

Standardized uptake values (SUVs) are a measure of the concentration of a radiotracer in a defined region of interest (ROI) divided by the injected dose normalized for the patient's body weight at a fixed time after tracer injection.

The cut-off value for malignant lesion is 2.5 [1] and it has largely been proven to be an oversimplification. SUV does provide an objective parameter for image analysis and is useful for research purpose. For patients with cancer, it is important to report SUV of chosen index lesions.

The Data and parameter for SUV calculation are stored in the DICOM file format. DICOM file is a file format developed by the DICOM Standards Committee whose members are also partly members of NEMA. The strength of DICOM files is the exchangeability between two entities that are capable of receiving image and patient data. DICOM also enables the integration of scanners, servers, workstations, printers, and network hardware from multiple manufacturers into a picture archiving and communication system (PACS).

Figure 1.2 The work flow diagram of PACS and DICOM in the system.

However, a specific application program is needed for reading the SUV. Each manufacture (vendor) have their own application, which is mostly supported just for their equipment.

Meirelles, et al.[2] have studied the comparison of the SUV by compare the SUV from the files that get through PACS (Picture archiving and communication system) and the files that view by the workstation at the scan site. The application program was used in their research is from the well-known vendor.

From the literature review and the study of the feature of DICOM format, we're interested in widening the limited condition by using MATLAB. It means that if we can use the widely used program such as MATLAB in PET DICOM analyzing process. It might be much useful for user.

DICOM file type is quite limited on viewing. There is seldom meet the application program supporting this type of file. The general photo viewing program in the market mostly not supports the DICOM file format.

Some application program has a feature supporting the DICOM file but only for displaying the image and the metadata, still unable to extract them to further process.

By the nature of the DICOM format, which contain by 2 parts, there are the part of image and metadata (Header) and MATLAB has a command that supports the DICOM file. Therefore in our research we choose MATLAB as a tool for calculation and analysis.

We have studied structure of PET/CT DICOM file and studied the various involved parameter in the method of SUV calculation. We found that DICOM file from different vendor is containing in different way. So in our research we used the DICOM file that process through the PET/CT Discovery STE from the GE healthcare[3].

For much understanding the meaning of DICOM file, the study of general meaning of the DICOM format from NEMA statement is needed[4]. Also combination study with the conformance statement from the vendor (GE healthcare)[5] has been studied. It provides the information about the way of storing parameter and the meaning of involved parameter.

After we reviewed the literature, we found that the SUV calculation from DICOM file was still not much prevalent.

Kanakatte and team[6] studied about the image of PET. They created the segmentation scheme to detect the tumor in the PET image. In their research they also use the SUV.

So our objective of this research is to study the SUV calculation from PET DICOM file by using MATLAB. For more practically in use, a performance comparison was tested with the Xeleris workstation, a well-known application in PET image analysis which is manufactured from GE healthcare.

CHAPTER II
CONCEPT & OBJECTIVES

1.1. Research Objective

1.1.1. Primary Objective

Create a new scheme of standardized Uptake Value (SUV) calculation from DICOM file by using MATLAB and compare the obtained SUV from the scheme to the Xeleris workstation.

1.1.2. Secondary Objective

- As a guideline for the SUV calculation from DICOM files by using MATLAB.
- To study the collection of data in a DICOM file, including the extraction of involved data for SUV calculation.

1.2. Research Hypothesis

H_o : Standardized Uptake Value (SUV) from the MATLAB's scheme and the Xeleris Workstation were not significantly different.

H_1 : Standardized Uptake Value (SUV) from the MATLAB's scheme and the Xeleris Workstation were significantly different.

1.3. Expected Outcome & Benefits

The SUV from the scheme which was created by MATLAB could be used interchangeably with PET/CT Xeleris® workstation. It can also be usedfor interpretation of PET/CT image without losing the capacity to accurately measure the SUV.

The new scheme is a stand-alone application, running on PC with MATLAB installing. Therefore, the new scheme allows for more simple interpretation of SUV. Physician can access, interpret and analyze data without other software.

The interchangeability of this scheme offers user to the convenient and approachability of data. The benefit of this scheme is that it can be adopted as a PET/CT analysis tool to medical imaging system. It allows a reduction in the number of computer for the practice. Moreover, it allows direct comparison with prior study without consideration of modality and its archive procedure, which is beneficial in a multi-vendor surrounding.

1.4. Research Place

Faculty of Medicine Siriraj Hospital
Mahidol University.
Bangkok, Thailand.

CHAPTER III
BACKGROUND & LITERATURE REVIEW

PET/CT is a hybrid system scanner that PET/CT plays an important role in medical imaging. It has been popular since it was launched to market in early 2001. The integrated PET/CT unit is to solve the problem of overlapping images on the PET image on CT image by reducing the movement of the patient. It simultaneously provides anatomical by CT scan that would help physicians to identify the anatomical position of the lesion shown on the PET image. So the integration of PET-CT has been shown to improve the accuracy of staging in cancer.

PET in the past has been employed to differentiate the benign from the malignant lesion. It also can be used for cancer staging as modal decision. Now the benefits of PET / CT in radiation treatment planning (RTP) has been widely accepted because of the ability to demonstrate the physiological data of the tumor cell. In the RTP, the tumor region and volume of the target lesion is important to prescribe the changing stage of lesion, so the accuracy of quantitative PET / CT scanner is also a big issue.

PET study begins with the injection or inhalation of radiopharmaceutical. The scan will start after delays ranging from seconds to minutes, to allow for the transportation and uptake by the organs of interest. When the radio-isotope decays, it emits a positron, which travels in a short distance before annihilating with an electron. This annihilation produces two 511 keV photons propagating in nearly opposite directions. If two photons are detected within the period of the coincidence timing window i.e. approximately 10 nanoseconds, a true coincidence event, if neither photon is scattered will be recorded along the two connected detectors which is sometimes identified as line of response (LOR).

3.1. Basic Physics and Instrumentation of PET

Positron is the anti – electron released during the decay of the nucleus of radioisotopes. Only Radioisotopes with an excess of protons may decay by electron capture or positron decay. During electron capture, one of the orbital electrons usually a k-shell electron is captured by the nucleus and proton nuclei is changed to the neutron. Electron capture can be written by

$$P^+ + e^- \rightarrow N + \nu + E \quad \ldots (3.1)$$

where P^+ is a proton, e^- is an electron, N is a neutron, ν is a neutrino, and E represents the excess energy released during decay. Process of electron capture isotopes cannot be imaged with a PET.

Radionuclides must be at least 1.02 million electron volts (MeV) more energy than the isotope to decays. Nuclear transition with less than this energy cannot undergo positron decay and only by electron capture. Radionuclides that have enough energy to step forward to the positron decay can decay by either positron decay or electron capture.

For the most commonly used PET radionuclides the probability of electron capture process is small enough that it can be ignored. In a few cases, an important fraction of the isotope decays by electron capture. i.e. ^{124}I , 74.4% decay by electron capture and 25.6% by Photon emission. Positron decay can be written by

$$P^+ \rightarrow N + \beta^+ + \nu + E \quad \ldots (3.2)$$

Where P^+ is a proton, N is a neutron, β^+ is a positron, ν is a neutrino, and E represents excess energy. Positron is the antiparticle that corresponds to the electron. Neutrino interacts very little with matter and it can be ignored for positron emission tomography (PET). The surplus energy is shared between the positron and the neutrino has different amounts of energy to each other during the decay of particles.[7-8]

The positron energy was lost in the tissue and forms the short-lived positronium with an electron in the tissue. In the tissue, Positron lost its energy from producing nearly two back-to-back photons of 511 keV (Fig.3.1).

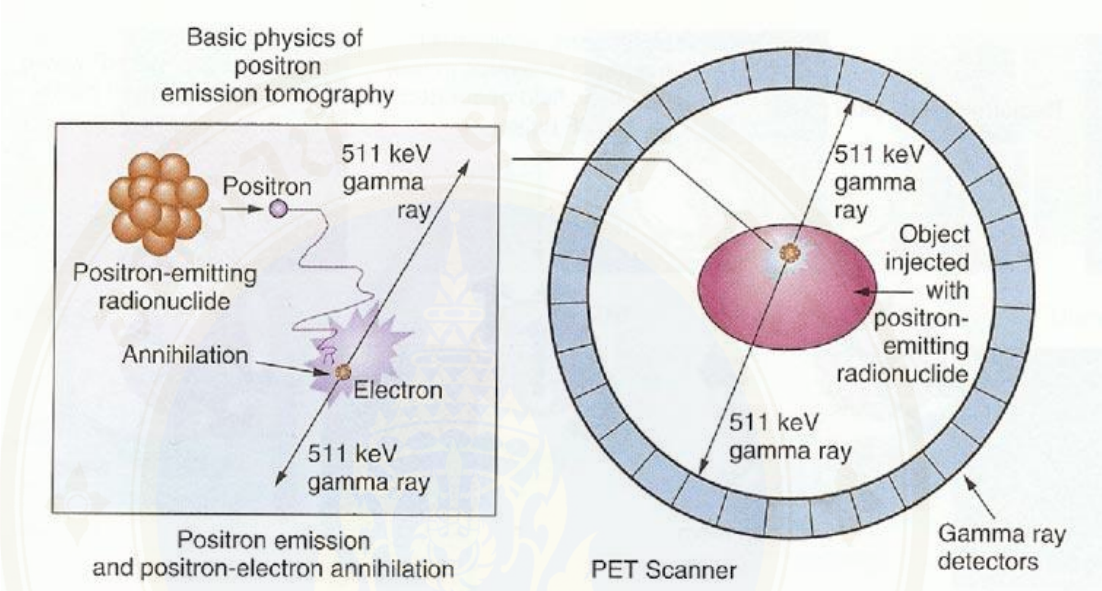

Figure 3.1 Basic physics of positron emission tomography.
(http://cellsighttech.com/technology/pet.html)

3.1.1. The Process of Detection.

PET/CT is a cylinder surrounded by a ring of detectors with a diameter of 80-100 cm and the range of 10-20 cm along the axis. The detector is protected from radiation from outside the field of view by thick lead shielding. Scanner working in the slice – collimated mode, the collimation axis is provided by thin ring called septa or collimator, which is made of lead or tungsten. In full 3-dimensional mode, the septa were retracted and can be collected during the pair inspection match possibly.

The two nearly back-to-back gamma is the key of PET. If the two detectors on opposite sides record an event at the same time, when the event destructive happened somewhere along the line between the two detectors. Two detectors are said to be "in coincidence", both events will be detected by camera almost the same time. The key of PET camera is an ability to identify the events that coincident occurred at the same time.

In PET, the imaging of the annihilation radiation are obtained from511 keV with co-linear (180^{o}) and simultaneously. Therefore, the measure of coincidence and ideally TOF (Time of Flight) measurement should be made. If a detector on each side record an event at nearly matching time, then the annihilation must have occurred on a straight line between the detectors. The straight line between the detectors is called the line of response.

Coincidence event is assigned to the line of response (LOR) joining the two involved detectors. In this way of the location information, it was received by detected radiation without physical collimator but electronic collimation is needed. Electronic has two main advantages, which are for sensitivity and uniformity improvements of the point source response function.

At the time that physical collimator is used. The directional data is receiving from photons that falling to the collimator that trap on the face of detector. In the collimation that was an electronic collimator, these photons are subject to inspected and used as a signal. The result is significantly in the sensitivity, typically for 2 D mode, a factor 10 for PET compared to SPECT mode. For the sensitivity increment, typical realizable image resolution in PET is around 5-10 mm, while in SPECT is approximately 15-20 mm.

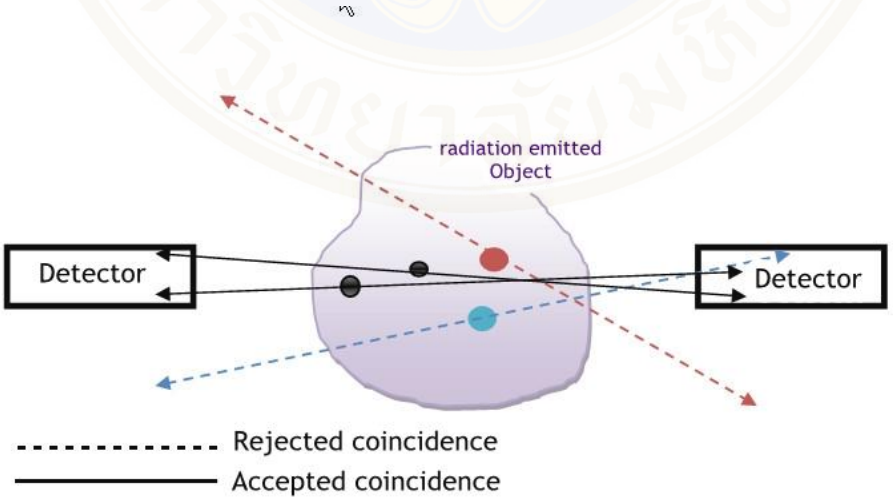

Figure 3.2 Accepted and Rejected coincident event from the detection

For detection of the incident as shown in Fig.3.2, a pair of gamma rays emitted from the tumor will be detected by corresponding detectors. In fact, cross-over time in the incident continually occur. Denote that the gamma rays from tumor are

emitted all times. During that time, double radiation may possibly occur. The mimic events that come from different sources might be the beginning of the error in interpretation of the further steps. So the window of time is used to improve the selection of the signal.

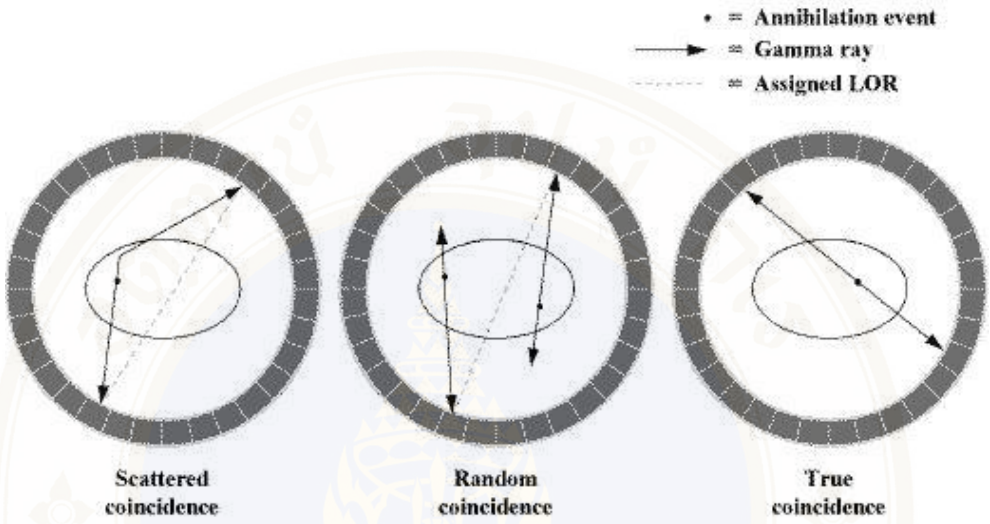

Figure 3.3 The coincident events in PET
(http://depts.washington.edu/nucmed/IRL/pet_intro/toc.html)

The coincidence events in PET fall into 4 categories: true, scattered, random and multiple. The first three of these are illustrated in Fig. 3.3

True coincidence is the events that occur when both annihilation photons reach detector without being scattered in the patient and both photon are detected. It is the most detectable event in PET scan.

Scattered coincidence is one chance in one or both photons are scattered. But both continue to be detected is called "scattered event", as shown in Fig.3.3 (1) these events are in the wrong location because the photon path is not on the same line. The Photons are at least one Compton scattering event happen before detection. Because the direction of the photons that have changed in the process of Compton scatter process. The events are likely coincident occur but it is defined as wrong LOR.

The coincidences add a background to the true coincidence that the distribution changes slowly with position, reducing the contrast and cause of overestimate the isotope concentration. It also added a statistically noise. The number

of events detected distribution depends on the characteristic and quantity of the being imaged, and the geometry of the camera.

Random coincidences occur when two photons arising from 2 events are not the same annihilation event but both records as an incident on the detector with the wrong LOR. The random coincidences occur where both events happen and fall on detector within the window time. The distribution of random coincidences is fairly uniform across the FOV and cause of overestimated the concentration of isotope if not corrected for. Random coincidences will be added statistical noise to the data.[9]

3.1.2. Detection

The detection and measurement of radiation depends on the interaction of radiation with matter. The concept of detection is the gases molecules interact with radiation and produce the negative and positive ions. The ions were collected by the voltage application. The ions are collected as current or count.

The amount of ionization is proportional to the amount of energy deposited by radiation. At low voltage, the measured ionization current is proportional to the amount of radiation. Dose Calibrators, pocket dosimeters and ionization chambers are all progression in principle at the low voltage (~ 150 V). At high voltage (~ 900V), ions are multiplied in that flood interaction. The pulse production is independent of energy and the type of radiation. The case of each interaction will be detected and counted, and this principle is applied in the Geiger - Müller (GM) counter which is used as a radiation survey meters. Detection of scintillation liquid work on the basis of the interaction of radiation with a special type of liquid that emits a flash when the interaction with radiation. Light will be processed in the same manner as in the case of solid detectors.

Both liquid and gas scintillation detectors are underperformance and validation. Therefore, they are not suitable used in PET technology, Interaction of radiation with a solid scintillation detectors is the basis of radiation detection technology in PET.

The feature of solid detector is unique. The property of emitting scintillation, sparkling glow or flashes of light after absorbing light or radiation, γ - X - ray light photons are converted to electrical pulse or signal by photomultiplier(PM).

Pulse will continue expand to the linear amplifier in order of pulse-high analysis (PHA) and registered as a count. Different types of radiation that is detected by various detectors. For example, γ - rays or X-rays are detected by the crystals of sodium iodide with the traces of thallium, NaI (Tl), while the organic detector such as anthracene and fluorplastics are used for particles detection.

PET is based on the examination of two 511 - keV photons in 180° coincidence. Photons are produced from the process of annihilation of positron-emitted radionuclide with electrons in the object (cell) and annihilated.[7]

3.1.3. Detectors in PET

Although many scintillation detectors have been reviewed, only some of them are acceptable for used in PET technology. The suitable of PET detectors depends on several characteristics such as.

- Stopping power of detector for 511 - keV photons
- The decay time of the scintillation
- Output light photons per keV of absorbed energy
- Energy resolution of the detector

When photons interact in crystal, electrons moved from the valence band to the conduction band. These electrons return to the valance band at synthetic capacity in the crystal, then emitting light in the process. Because impurities usually on meta stable excited state, the light decay rate spells out the characteristic of crystal exponentially.

The stopping power of the detector resolves the average distance photons travel through the rich accumulation of energy and depends on the density and effective atomic number (Z_{eff}) of the detector material.

Scintillation decay time occur when atoms interact with the γ ray detector materials and atoms are excited to higher energy levels which subsequently decay to the ground state, emitting visible light. the production of 2-60 light photons per keV of energy that occurs depends on the type of material detected.

The time of decay is called the scintillation decay time given in nanoseconds (ns) and varies with the material of the detector. The shorter decay time

is the higher efficiency of the detector at high count rates. A high-light-output detector produces a well-defined pulse resulting in better energy resolution.

High-density is an ideal crystal, the good stopping power is a characteristic that give high light output with an accuracy of positioning when detector hit by a large fraction of photons, fast rise-time for accurate timing, and a short decay time so that high counting rates can be handled. Most scanners currently used bismuth –germinate (BGO), which generates about 2500 light photons per 511 keV photon and decay time of 300 nanoseconds.

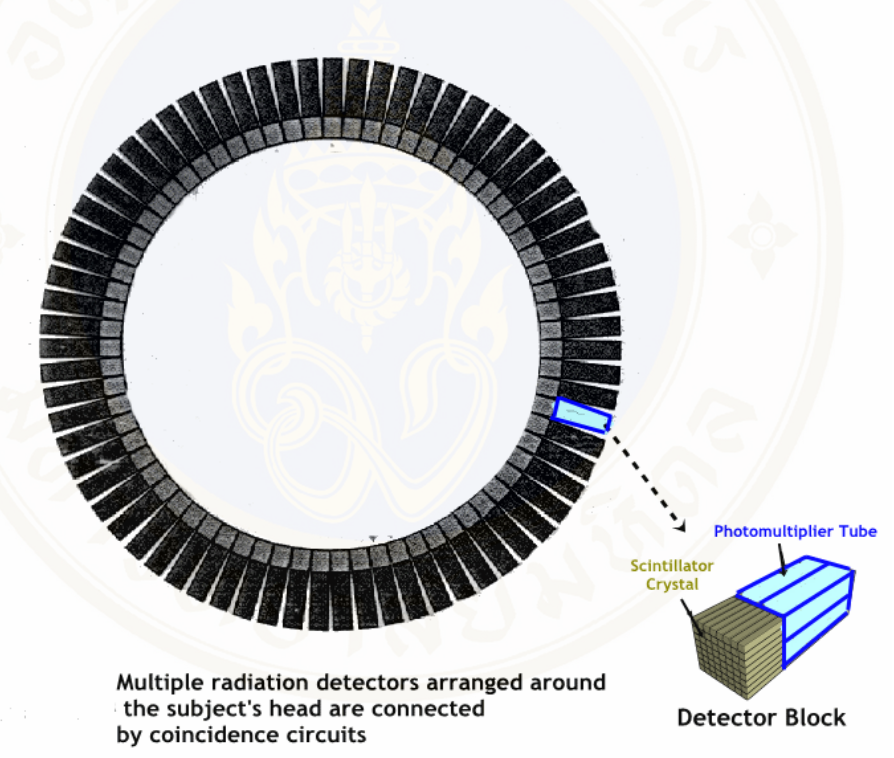

Figure 3.4 A block of BGO crystal separated into 64 individual detectors but coupled to only four PM tubes. The location of γ-ray interaction among the 64 detectors is determined from the pulse height distribution between the four PM tubes.

A block is often constructed from many scintillations crystal but lesser of photomultiplier tubes. A set of the ring is made up from several blocks, and then the total number of coincidences between crystals is proportional to the square number of crystals. In cameras with around ten thousands of crystals, it's quite complex

electronic. So the coincident circuit may identify coincidences between two blocks rather than between each crystal individually. After the incidence is determined, the individual crystals are prescribed by the logic of anger, and only line of response is determined by a computer. If the incidence is not detected, then other steps in the audit do not need to be performed.

The design of detector as block can help with servicing. Hardware problems can be relatively easily modified by changing a single block. This is important especially at the beginning of the development of commercial systems. Disadvantages of block design are that there may be differences in the properties of the detector center and the edge of the block. Some are not present in the physical block, but they are still thinking in defense of detectors for the detection of coincidence. [7]

3.1.4. Photomultiplier Tube (PMT)

As discussed briefly earlier, the large crystal size coupled with the multiplier tube (PMTs). The block is fabricated in a manner that the amount of light collected by a unique difference to each PMT depends on crystal scintillation occur. Therefore, integration of the PMT can decode the output of each scintillation position light. The total sum of PMT output is proportional to the energy accumulated in the crystal.

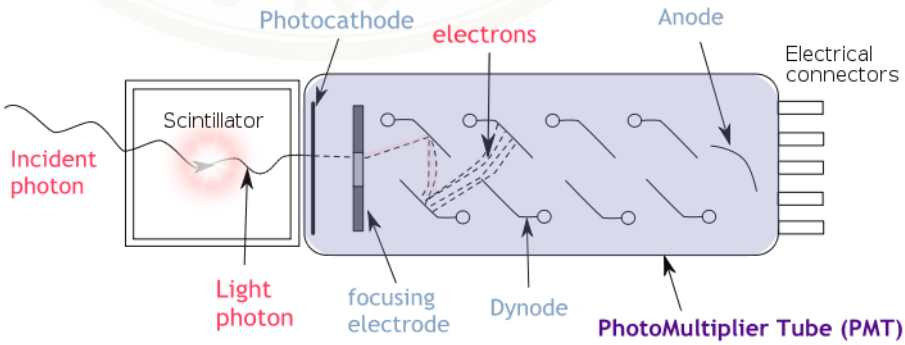

Figure 3.5 The PMT

The PM tube in Fig.3.5 is a vacuum glass tube with a photocathode at one end, ten dynodes middle and anode at the other end, photocathode is usually the alloy

of bi-alkali materials i.e. cesium and antimony give electrons that came out after the absorption of photons.

PM has been fixed to the detector by optical lubricant or light pipe. High voltage of ~ 1,000 V will be used between photocathode and anode with respect to increments between dynodes when light photon from detection strikes the photocathode, then electrons emitted, which are accelerated toward the next to dynode by the difference the voltage between dynodes.

Around 1-3 electrons emitted 10-70 individual light photons. Each electron can be accelerated again to the next dynode and emitted more electrons. The process of multiplying until the last dynode of the electron pulse and the electron pulse is now millions of times larger than it was at the beginning of the tube. At this point the electrons are collected by an anode at the end of the tube forming an electronic pulse. Pulses sent to a preamplifier will be next expanded by the amplifier to a pulse as high as can be detected. Then the analysis of it size will operate by PHA, and deliver finally to recorder or computer for storage or display monitor. The PM tubes are well-built and expensive but provide fast and strong output pulse.

A group of photomultiplier tubes views the flash of light from the scintillation in the crystals from the amount of light relatively distributed to each phototube. The position of the scintillation light can be determined.

Each scintillation produced a large number of light photons, around 10,000. Scintillation moved from the crystals on the side of the crystal blocks in other side, the ratio of photons in the tube varies. This ratio can be used to identify the scintillation in the crystals. [10]

3.1.5. Pulse Height Analyzer (PHA)

The Number of photons produced a scintillation light proportional to the energy of the incident photon and the charge in the photomultiplier tube. Therefore, the electrical signal coming out of the detector is proportional to the energy of incoming gamma rays. These signals are passed through the pulse high analyzer, which allows only the proper energy.

It is fewer occurrences a signal that higher than 511 keV, and usually that higher energy produced by a combination of the 511 - keV photons and low energy

photons scatter. In such cases it might be desirable to create that with 511 - keV events and ignore the lower signal. Therefore, the pulse height analysis is often used only as a discriminator for the upper and lower-level. Raising the lower-level discriminator will reduce the number of scattered photons that are counted as photo peak events. If the lower-level discriminator is raised too high, then true coincidence events will be lost.

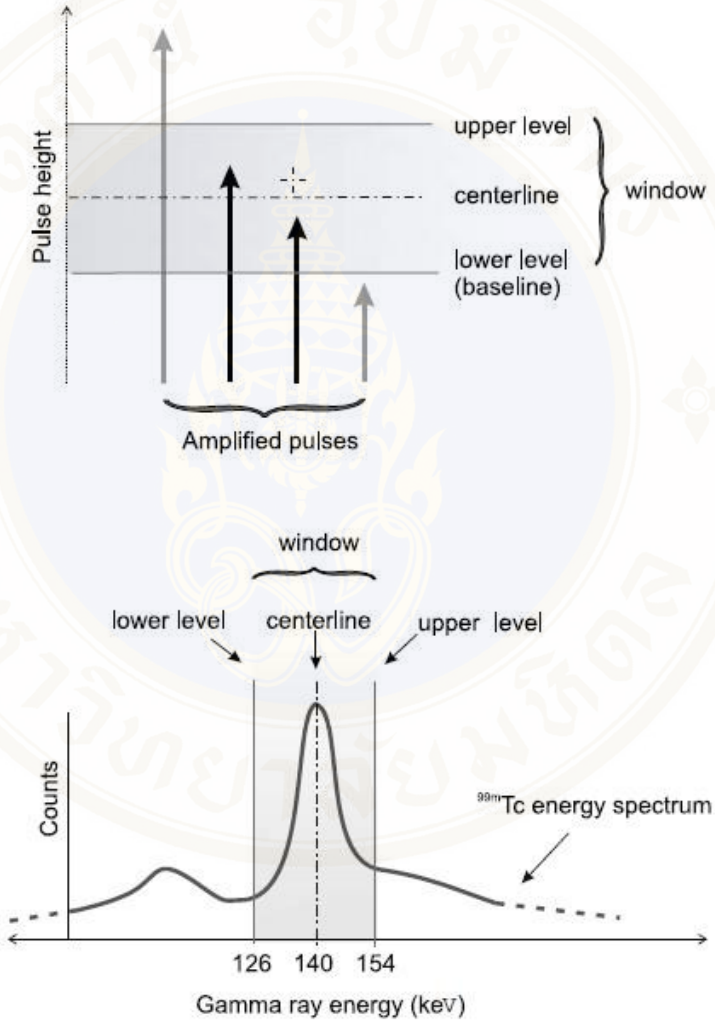

Figure 3.6 Pulse-height analyzer. The incoming pulse is proportional to the energy of the initial gamma ray photon. The pulse-height analyzer accepts only those that fall within the window. [11]

Improvements in energy resolution will improve efficiency by providing better separation of photo peak and selection of lower level discriminator is more complex. An annihilation photon may build it to the crystal, scatter in the crystal, and

the secondary photon may run off. Because photons are not scatter within patients, these events will represent actual events. However, they deposit less energy in the crystal. Photons that go through in high angle scattered within the crystal can result in a pulse that is very close to the scatter in patients, so lowering the discriminator in the lower-level may actually both increase the number of true coincidences (the scatter in the crystal) and bad coincidences (which are scatter to patients). [7,11]

3.1.6. Collimator

We assume initially that data are collected with standard gamma camera fitted with a conventional parallel-hole collimator. To simplified the analysis, several assumptions are made. We consider only a narrow cross section across the detector. The collimated detector is assumed to accept radiation only from thin slice directly perpendicular to the face of detector. Each collimator hole is assumed to accept radiation only from a narrow cylinder defined by the geometric extension of the hole in front of the collimator. This cylinder defines the LOR (line of response) for the collimator hole (Fig.3.7).

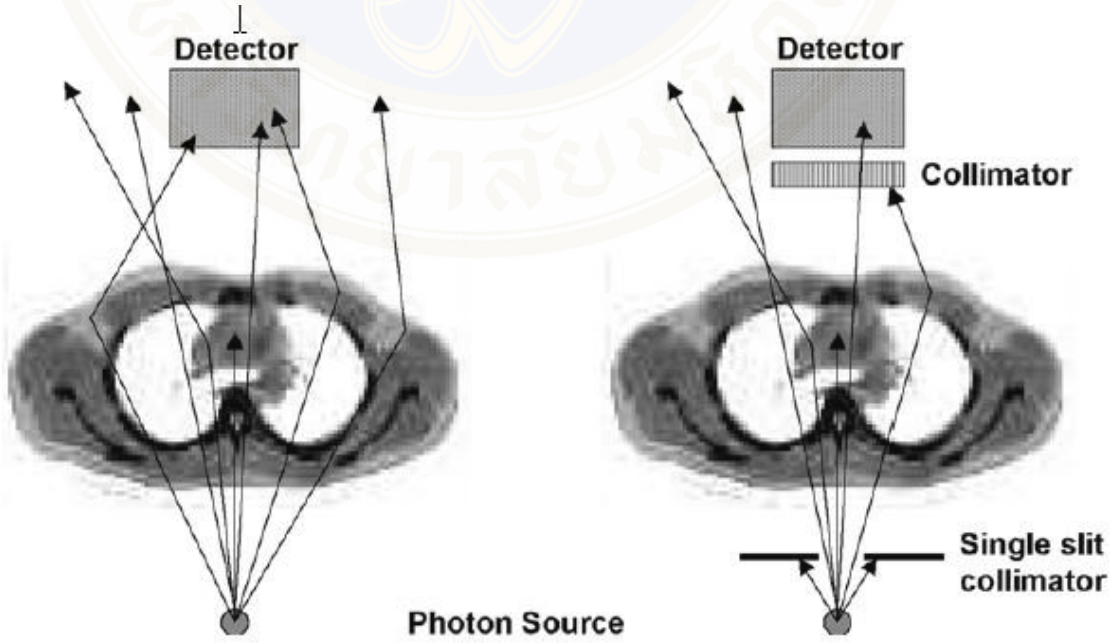

Figure 3.7 Each collimator hole views the radioactivity within a cylinder perpendicular to the face of gamma camera, call its "Line of Response". [8]

3.1.7. Data Acquisition for PET

PET imaging modalities, along with several other images can be explained with a model of the line-integral. We begin by considering the parallel piped joining any two detector elements as a volume of response

In the absence of physical effects such as attenuation, accidental coincidences and scatter, variations of effectively detector or count-rate dependent effect, the total number of events that happened detected is proportional to the amount of tracer contained in the tube or the volume of response (VOR).

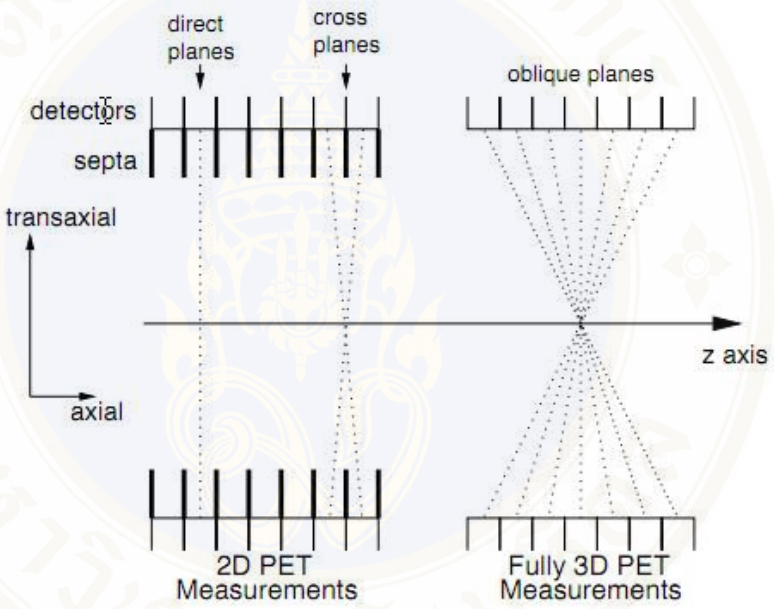

Figure 3.8 The acquisition of data in 2D and 3D.[12]

3.1.7a Two-Dimensional Imaging

PET scanner mostly design with collimators or septa, that installed between each ring of detector. The collimators allow only photons that emitted parallel to the detector plane (Fig.3.8). Only that case will be detected. This is how 2D acquisition mode start working.

The collimator will reject many annihilation photons that have been scatter in the body, reduce the single-count rate and minimize dead time losses.

Each crystal ring collects the data from a single slice while oblique lines of response are not allowed because of collimator. The 2D projection

data are analogous to the data obtained with a rotating gamma camera with parallel-hole collimator that was used in SPECT imaging. Therefore, the image can be reconstruction by using the filter back projection or iterative algorithm.

3.1.7b Three-Dimensional Imaging

As describe above, the multislice 2D data acquisition by reject any photon that have an oblique line. This is very wasteful because many potential annihilation photons from coincident events are absorbed by collimator.

In 3D acquisition mode the collimator are removed from the face of detector plane. So data will be obtained from all possible line of response. From that condition lead to well improve the sensitivity. The number of scatter photon and the counting rate are also increased.

In 3D mode, it is important to place the structure of interest as close as possible to the center of FOV. 3D is widely used for brain scan. The reconstruction of 3D data is also more complex because they cannot be sort in to a set of independent 2D slice. Therefore both Fourier-based and iterative were used to reconstruct the data in 3D mode.

The computation times of 3D mode are longer than the 2D mode. However the 3D acquisition is available on all commercial PET system and in some image center used 3D as a standard mode.

3.1.8. PET Image Reconstruction

In transverse slice using iterative algorithm. Sagittal and coronal slice are reconstructed from transverse slice.

Iterative reconstruction is steadily replacing filtered back projection. Iterative reconstruction starts by estimate data to produce a set of sliced. These slices are then used to create the next (second) of projection views by compare to the original projection views that was acquired from patient at the first step. The transaxial slices are then modified using the difference between 2 sets of projection. The estimation keep processing as a loop as shown at diagram in Fig. 3.9.

The process is complete when the difference between the projection views of the estimated data and original data is below a pre-determinate threshold.

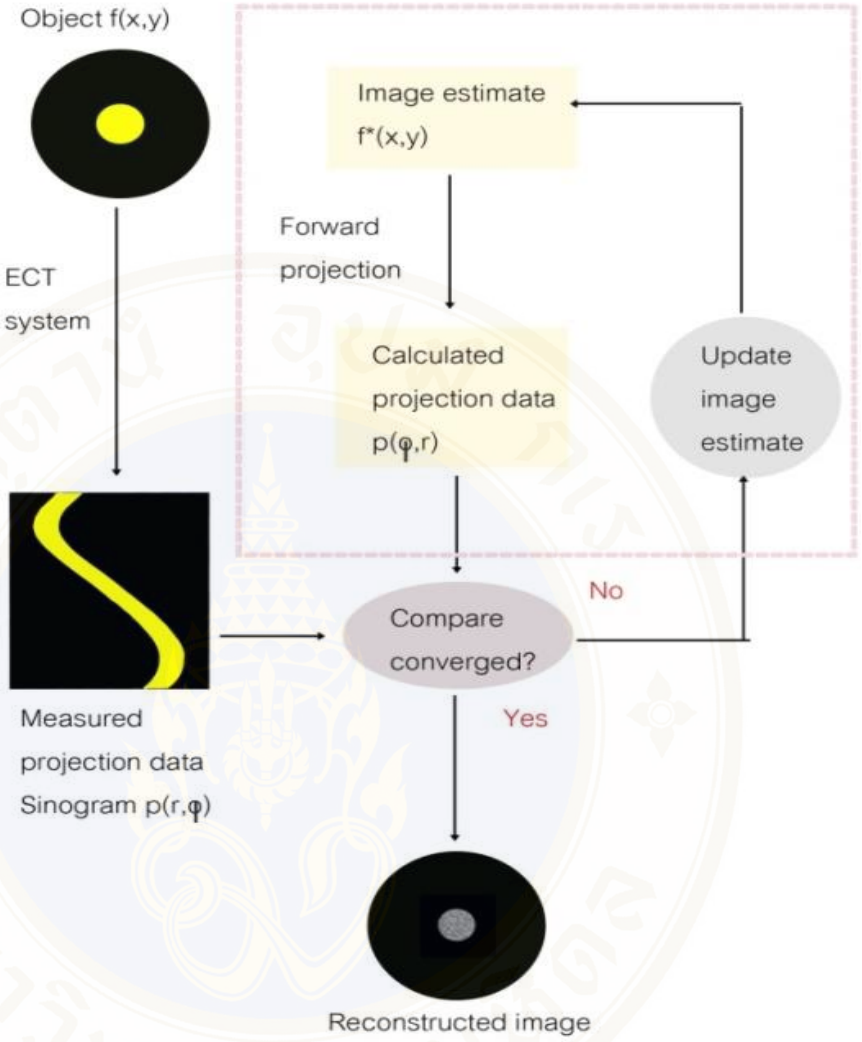

Figure 3.9 Iterative Algorithm Processing

Advantage of iterative reconstruction are good image quality, less star artifact as seen in back projection technique, and correction for attenuation, scatter, and even collimator

Currently, the use of iterative reconstruction is unlimited because of high technology of computation.[12]

3.2. RADIOPHARMACEUTICAL

PET is a non-invasive diagnostic tool that provides tomographic images and quantitative parameters of the blood perfusion, cell viability, proliferation and / or metabolic activity of tissues. These images result from the use of different substances of biological interest (glucose, amino acids, and hormones) labeled with positron emitting radionuclides.

In this research we will focus on the F18-FDG, which used widely in the PET imaging in oncology.

3.2.1. F18 production by Cyclotron

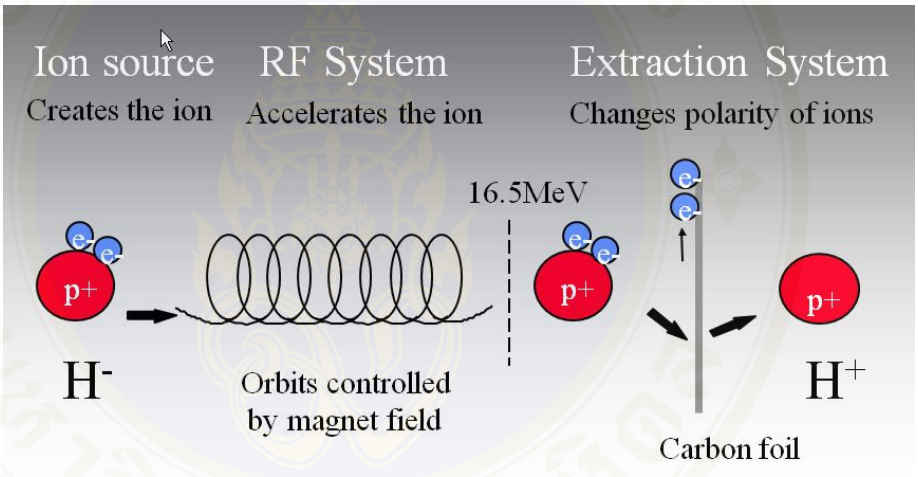

Figure 3.10 After acceleration, the Beam Extraction by thin carbon foil placed at extraction radius. Electrons are tripped off "Ion become Positron" (remove the "-" e- in the case of F-18 production.

F-18 target in the cyclotron is bombarding to the O-18–enriched water. Negatively charged hydrogen ions are accelerated in a cyclotron till they gain energy about 8 MeV or more (Fig.3.10).In the extraction system orbital electrons are removed and resulting high-energy positive ions of hydrogen (H), or proton beam is directed to a stable target chamber that enclose the O - 18-enriched water molecules (Fig.3.11). The nuclear reaction of Proton and the O-18–enriched water form the hydrogen (F - 18) fluoride is given by

$$H_2(O-18) + (H-1) + energy \rightarrow H_2(F-18) \quad \ldots (3.3)$$

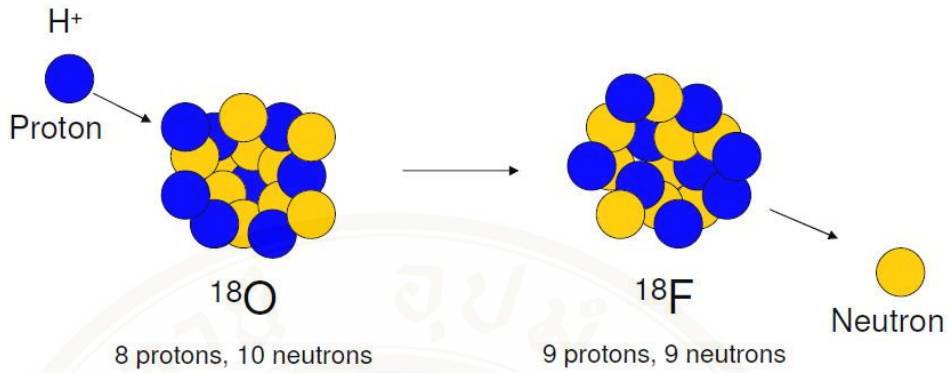

Figure 3.11 F18 production by cyclotron

O-18 and F-18 are isobars, that is, they are same mass numbered (A =nucleons) but different atomic numbers (Z is 8 for oxygen and 9 for fluorine). F - 18 is an unstable radioisotope with a physical half-life of 109 minutes, it decayed by the emission of beta - Plus or electron captures and emits a neutrino (υ) and a positron (β^+):

$$F - 18 \rightarrow O - 18 + \beta^+ + \upsilon \quad \ldots (3.4)$$

Positron release energy in the form of coincident photons by annihilates with an electron. It happen by changing the molecule in the target chamber, otherpositron - emitting radionuclides such as C-11, N-13, and O-15 also can be produced.

$$\beta^+ + e^- \rightarrow \gamma\,(0.511\ \text{MeV}) + \gamma\,(0.511\ \text{MeV}) \quad \ldots (3.5)$$

The O-18 rich water in container is the target for production of F – 18. It was produced under standard conditions by using the cyclotron, varying the amount of O-18 enriched water in container takes vary processed time**.**

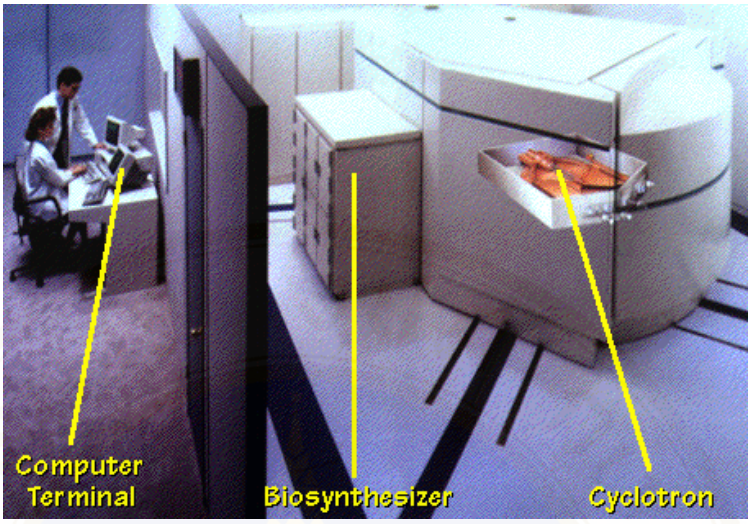

Figure 3.12 Production of F18-FDG in work area.
(http://www.cerebromente.org.br/n01/pet/petcyclo.htm)

3.2.2. F18-FDG Synthesis

PET radiopharmaceuticals are used for diagnostic used for imaging of metabolic pathway in the body. More progressive PET technology is employed for drug development and drug discovery. A short life commonly used in PET is F-18, the fast syntheses of the F-18 radiopharmaceuticals is needed.

Microfluidic devices are mostly used in order to improve time, yield and safety.

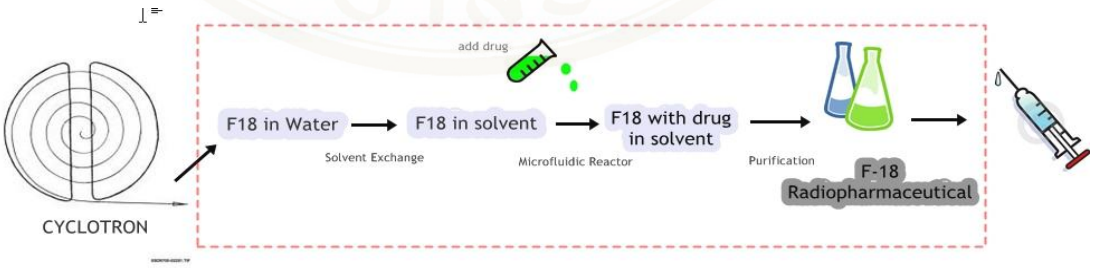

Figure 3.13 Step of F18-FDG synthesis

After bombarding O-18 enrich water with protons in the cyclotron provide a mixture of H2 (F - 18) and O - 18 - enrich water, an automated computer-controlled mixture is a process which takes about an hour to complete the FDG production. The sterile liquid non-pyrogenic, colorless and clear was yields with a solvent that is less

than 0.04%, The purity of radioactive materials is greater than 95. % and the activity was about one 35-50% of the original activity.(This process may vary depending on radiopharmaceutical).

An imaging functionof PET may take many forms. Although it started in the laboratory by using a variety of radioisotopes such as 14-Clabeled deoxyglucose, but widely used techniques that are in clinical practice today is F18-FDG.[13]

3.2.3. F18- FDG PET Imaging

FDG could be used as tracer for diagnosis of cancer because FDG is an analog of glucose that the living cell will be taken up in the first stage of glucose pathway. The taking of FDG by cell depends on an increased of glycolytic activity in neoplastic cell.

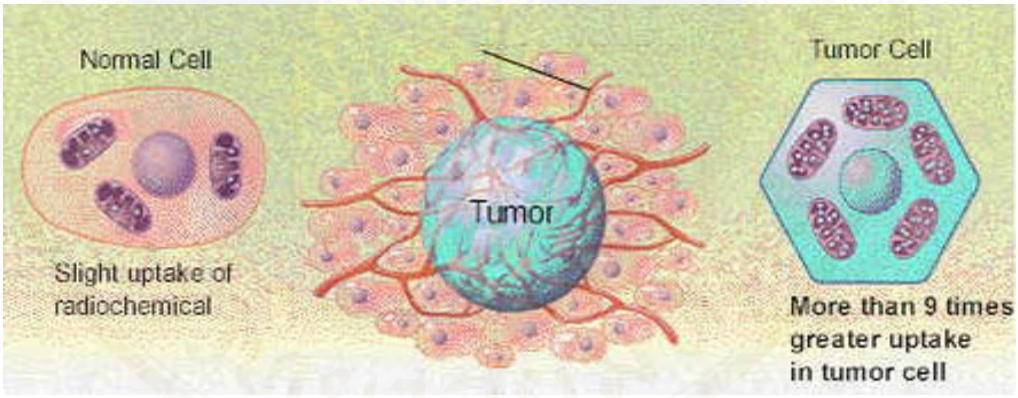

Figure 3.14 Fluorine-18 FDG, is used to locate tumorous cells.
(http://mdti.us/MDTI_faqs.htm)

FDG is trapped in to the cancer cell, that have high glycolytic activity and with no excretion from the body through the renal system. Time taken interval between FDG administrations to scan is approximately 50-60 minute, that usually enough for obtained a good image.

The changes in cells associated with the neoplastic transformation correlated with impaired function that apparent before structural alterations occur, so FDG PET can reveal the presence of tumor when general modalities such as X - ray, CT, MRI and ultrasound has not been clearly detected. FDG uptake in tumors associated with the growth of tumors and viability, so PET scans and the metabolism

provide useful information about tumor characteristics, prognosis of patients and monitoring the cancer therapy. Currently, much and more evidence show that the application of FDG - PET is becoming more and more widely for diagnostic and evaluation of patients with suspected cancer, in staging the tumor and the treatment is reviewed. For the moment, interest is growing in the capability of using a variety of F18 radiopharmaceuticals for research other than oncological imaging .

3.3. STANDARDIZED UPTAKE VALUE (SUV)

Other significant benefits of molecular imaging are ability of monitoring the metastasis and response of the tumor to the radiation. The metabolism and uptake of PET radiopharmaceuticals was quantified and referred to the patients, through the semi-quantitative analysis.

In semi-quantitative method, static images in the illustration of tissues are evaluated to determine and compare the relative uptake in tumor. The ratio of tumor to normal tissue activity ration (T / N) are used but not prevalent, It is using data from normal and tumor region in the reconstructed image. The Ratio does not depend on the amount of injected dose, patient weight and the blood sugar level. But the critical of corrected reference is an area in abdomen and pelvic.

The most versatile semi-quantitative technique is the standard uptake value (SUV) method that is widely used in nuclear medicine and molecular imaging

PET scan is affected by the scatter, attenuation and random. However, all these effects can be accurately corrected. The distribution of activity was correctly shown in the final PET image. To obtain a complete quantity of activity, a measurement of a known source activity is needed. From the calibration of the PET/CT machine, corrected value can decode the count rate into activity. From the known source scan, and attenuation corrected image can be converted in to activity per volume (MBq/cm^3).

Standardized Uptake Value (SUV) is universally used in routine clinical practice. It is used as parameter of the semi-quantitative in FDG - PET analysis. The SUV provides a determination of activity in a defined region of interest (ROI)

normalized to the patient's body weight and administered dose. Being a ratio, it is unit less and is calculated by

$$SUV_{bw} = \frac{\text{Measure Activity in Region of interest (ROI)}_{(mCi/ml)}}{\frac{\text{Injected Dose}_{(mCi)}}{\text{Body Weight}_{(g)}}} \quad \ldots(3.6)$$

To calculate the SUV, ROI was drawn on the image that was appeared on the screen by the reader (physician). The computer then calculates the average density or maximum density in that ROI, then the decay of uptake in the period and counting efficiency were corrected. The pixel intensity value in the ROI area finally was converted to the activity per gram of tissue, assuming tissue density is equal to 1 g/cc. The body weight (kg) and injected dose (μCi(Bq)) were together used, the SUV is calculated for the ROI using Eq. 3.6.

If the PET scanner has been calibrated, then the technologist only needs to enter the patient's weight, the administered dose in the application's workstation, and then the time the dose was measured.

Basic ideas of SUV are that if the activity is uniformly distributed over whole patients and no excretion, the SUV will be equal to "1". [7]

SUV measurements are overestimated by the above formula ($SUV_{body\ weight}$) in patients who are overweight because fat does not concentrate FDG as much as the rest of the tissue of the body. The contribution of the patient's weight towards the SUV is reduced if the patient body surface area (BSA) is used in the calculation instead of body mass. This is because the formula for the calculation of the BSA incorporates the patient's height as well as his weight. BSA is estimated by

$$BodySurfaceArea = (weight_{kg})0.425 \times (hight_{cm})0.725 \times 0.007184 \quad \ldots (3.7)$$

The formula for SUV based on body surface area becomes

SUVBSA = (calculated activity in the region of interest) × (body surface area)/(injected activity) … (3.8)

Wang et al.[14] described the 18F-FDG uptake in normal tissue. This study maps the distribution of 18F-FDG uptake in organ of patients with no abnormalities in those tissues. They described how physiological uptake varies with factor such as age and sex. This paper presents extensive data on patterns of physiological FDG uptake in normal tissues throughout the body, which if used as an adjunct to physician experience in PET/CT image review.

In the SUV according to **Thie**[1],the author collected and discussed about the factors directly affecting SUV , the confounding factors influencing SUV determination of defined tissue type and state for defined population of patients. Moreover, Factors affecting SUV was classified into 3 parts. 1) Tissue activity factors (ROI shape, partial-volume[15] and spillover effects, attenuation correction, reconstruction method and parameter for scanner type, counts' noise bias effect).2) tissue state factors amenable for correction. Many biologic factors determine a particular tissue's uptake such as kind and extent of disease, vascularity, organ usage, urine management policy, population characteristic and so forth. Among such conditions at scan time, only 2 are singled out as candidates for SUV correction. There are time of SUV evaluation and competing transport effect.3) normalization factor (body size). This study also has described the methods and implication for usage of SUV.

The SUV is particularly useful when comparing between different experimental study results. It provides a quantitative number, which can easily be compared. In clinical practice, it is used less commonly. Generally, clinicians use the internal control of image intensities, e.g., comparing pulmonary nodules to the mediastina blood pool. However, even in clinical practice when it is readily available it can be useful to help consistency from day to day.

SUV is affected by several factors. It has a strong positive correlation with weight if calculated the SUV in body weight term. Also image noise, low image resolution, user biased ROI selection, time of measurement is also effected, the earlier imaging provides low results, and conversely delayed scans provide high SUV. Also the other factors such as dose extravasations, attenuation parameters, reconstruction parameters, partial volume effect and plasma glucose level in patient blood affect the value of SUV. In summary, SUVs are a convenient measure for the evaluation of

dynamic FDG-PET images, but need to be taken with respect to its pitfalls and interpretation of the results.

Among the factors that affect SUV issue, **Boellaard et al.**[16] have varied several parameters without intention to address the biologic factors influencing the denominator of SUV calculation. The parameters varied are the type of ROI, the presence or absence of spatial filter for one particular reconstruction algorithm, the noise equivalent counts collected, the number of pixels reconstruction matrix, uniform spherical lesion size and the lesion-to-background ratio. Results showed that SUV depended on all parameter studied. The poor accuracy of the SUV under various condition may hamper its use for diagnosis. Therefore, the SUV might be more suitable for response-monitoring purpose.

Ivanovic et al.[17] they performed a study to evaluate the effects of PET acquisition parameters on calculated SUV_s for the same lesions. They investigated the effect of varying total counts in the lesion to background ratios, 2-D versus 3-D imaging geometry (lesion position in the image). They also evaluated the differences in SUV_s for the same lesion in image reconstructed using FBP and OSEM with variable number of iterations and subsets. The results showed that the variation in the calculated SUV_s as the function of selected acquisition and processing parameters in addition to the variation due to patient dependent parameters indicated that distinguishing between benign and malignant disease based on SUV_s, and using SUV_s as semi-quantitative parameter in follow-up studies has to be interpreted with caution.

Ivanovic et al.[18] showed the dependence of SUV on imaging protocol for dual time point. They demonstrated the large variation in the calculated SUV as a function of selected imaging protocols with different acquisition and imaging reconstruction parameters.

One more factor that affecting SUV is the time after injection. Understanding how SUV changes in tumors over time after injection is useful for comparing varying times between injection and PET imaging, thus improving the useful of 18F-FDG SUV when comparing different studies, including serial studies in the same patient.

Beaulieu et al.[19] measured the SUV changes with observation time after injection in breast cancer. In this same paper they examined the feasibility of an

approximate method to compare the SUV_s from studies with modest variations in the time between injection and uptake measurement experienced in clinical practice. ^{18}F-FDG was performed as 60-min dynamic imaging with an additional image acquired at ~75-min after injection. Both the maximum SUV and the average SUV within the lesion were calculated. The rate of SUV change with time was compared with the instantaneous SUV obtained at different time from 27 to 75 min. This paper concluded that the time dependency of 18F-FDG SUV stresses the importance of consistently acquired images at the same time after injection. However, if this cannot be achieved in busy PET department, the method for adjust time of uptake in this paper could be applied.

Sajdak et al.[20] they present about technical factors affecting the SUV calculation for FDG PET. In this study errors from the PET scanner and from factors under the technologist's control were limited to within 20%. It showed that technical factors should not be neglected. Attention to technical detail is the key to accurate calculations of the SUV_s.

All these literatures above are the example of publications which have been discussed about factors affecting SUV. In the next section, there will be the literatures which focus on the method of SUV measurement, the accuracy and reproducibility of SUV.

In PET imaging SUV_s are used as an indicator to determine whether tissues and organs are within normal ranges. However, there is great variation from patient to patient and physicians sometimes concerned that the measurement is not accurate. Routine measurement of SUV in the phantom reassures the system is working correctly and that the SUV_s are properly determined by system.

Minimizing errors in SUV measurements require imaging studies to produce reliable results that can be used to access disease status. Since data acquisition and reconstruction are performed in many different settings and often with different types of instrumentation. Standardization of image acquisition protocols is one important approach for addressing this problem. It is important that the image instruments are performing according to the specification. The American College Radiology Imaging Network (ACRIN) PET come laboratory was initially developed to ensure that individual PET scanners were properly calibrated and were being

operated in accordance with manufacturer's recommendations and guidelines. The **ACRIN protocol** [21] has described the quantitation procedure for PET and PET/CT imaging, the method of measurement and the required uniform phantom. The uniform phantom image can be obtained with a fillable phantom containing F-18 detected in water or with a $^{68}Ge/^{68}Ga$ solid phantom.

More detail about PET phantom was described in the ACRIN PET phantom instructions for evaluation of PET image quality.[22] This booklet is to be used by the facility applying for accreditation in PET imaging. It contained the basic information about phantoms, preparation of phantom, data acquisition and processing, and basic region of interest (ROI) analysis.

Zanzonico[23], reviewed routine quality-control (QC) procedure for all current nuclear medicine instrumentation including PET and PET/CT scanner. The procedure described and their respective frequencies were presented only as general guidelines.

Gong et al.[24-25], performed the standardized quality control procedures to monitoring the PET scanner using uniformity phantom ($^{68}Ge/^{68}Ga$solid phantom). The following study was performed for comparison of two PET system (Hybrid PET/CT and Dedicated PET)**.**The accuracy and reproducibility of SUV were analyzed.

3.4. DICOM

Software is provided from commercial vendors for the acquisition, processing, storage and display. It is specifically designed for their scanners. Such software was either developed by a vendor or from the third-party software developers. Type of software that uses a proprietary format of each vendor and it is difficult to transfer, store and display images on devices from different vendors.

This problem can be solved partially by using all the devices from the same manufacturer in the institution. To overcome this difficulty, American College of Radiology (ACR) and National Electrical Manufacturers Association (NEMA) jointly support the standard format for software known as DICOM.

DICOM stands for Digital imaging and communications in medicine.

DICOM is not just an image or file formats. It covers all of the data transfer, storage and display protocol created and designed to cover all aspects of digital photography, medical simplified. It seems that every company with a DICOM plug into their networking names PACS (Picture Archiving and Communication System).

The PACS is a medical system for storage of images and transferring images between computers in different facilities through networks. This system consists of necessary hardware and software to produce (modalities – such as computed tomography (CT) scanners, ultrasound, or PET/CT)and digital image archives (store digital images electronically), workstations(where radiologists view the images) to view and interpret images, and a network linking computers from different sites. Appropriate PACS software allows the interpreter to manipulate images as needed, at his own location. [26-29]

PACS is a connection between computers through a network of high-speed data sharing. This connection can be in the division by using a local area network (LAN). In a hospital using an intranet or outside the hospital using the Internet, PACS will be helpful to make a comparative study, such as shooting at different among modalities through Web protocols without having to physically move to and from different locations of the department. Similar to the image transfer, that may occur through the PACS to other parts of the hospital, also to various parts of the country or even to other countries.

The goal of PET/CT using as the method of quantitative evaluation reflects the biological behavior of tumors. The accuracy of these quantitative values is important for targeting. Decisions about the treatment of patients caused a significant effect on the quality of his or her life. PACS should not distort data. Many researches are interested in the related with and without PACS.

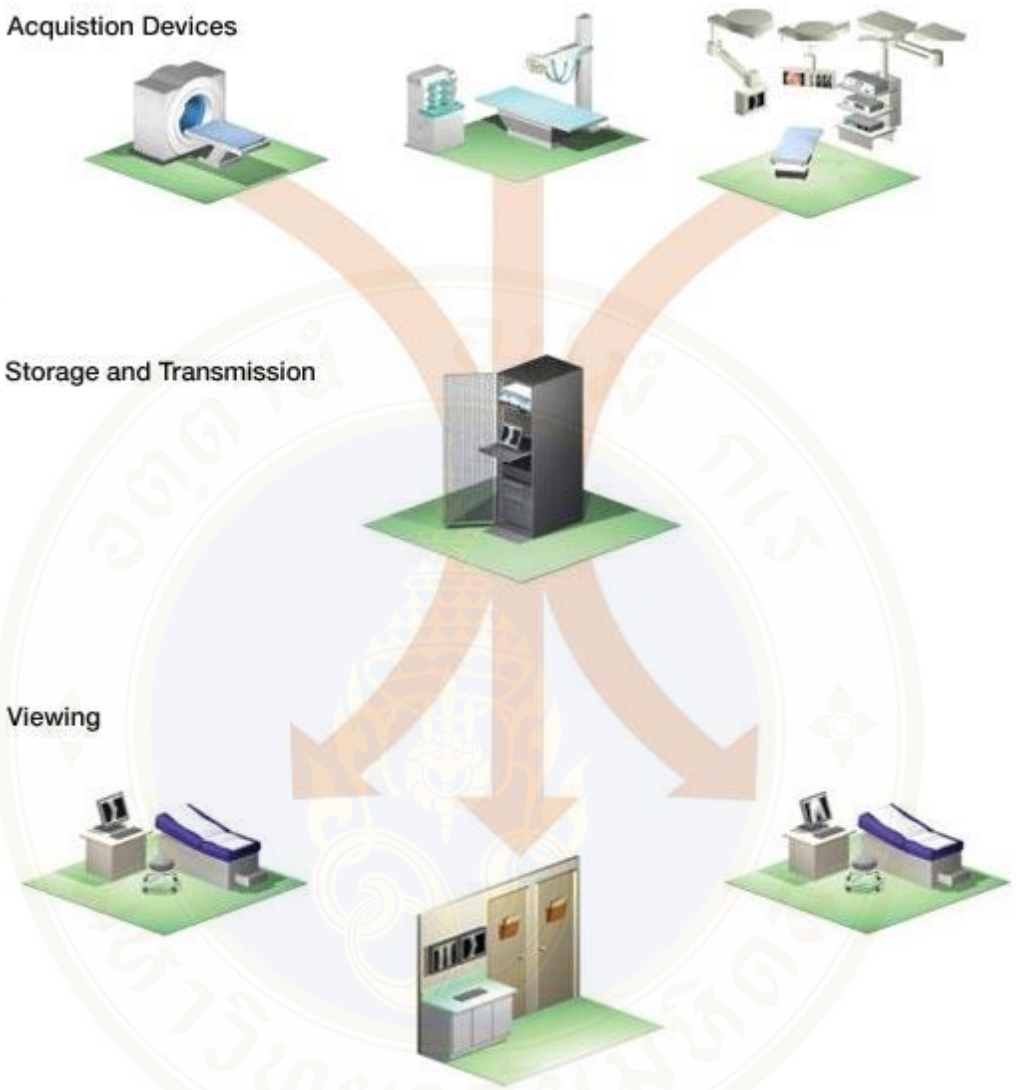

Figure 3.15 Major Picture Archiving and Communication System (PACS) components. Image acquisition devices (modalities) store images on a digital archive. From there images are accessed by radiologists at the viewing workstations. (http://www.stryker.com/cn/Solutions/KneeReplacement/PACSSoftware/006025)

The Quality Assurance and Quality Control which reviewed in last section regard as important rule for quantitative data analysis. The SUV values are important predictors of outcome in malignancy diagnostic and the present time PACs also play a role in radiology information system, therefore many study interested in the SUV and PACs

In the correlation between SUV and PACs according to **Meirelles et al.** [2], the researcher put one of these PACs modules to the test by comparing it with SUV measurement from two vendors' dedicated PET/CT workstation. The PET/CT images were reviewed by radiologist at the manufacture's dedicated workstation for the modality. GE Healthcare's Xeleris and Siemens'sSyngo. The image from all the FDG studies were also reviewed on the facility's GE Healthcare Centricity PACs with the Volume Viewer Plus module.

In the next review is the examples of other type of digital images, which has been reviewed and analyzed through PACS compare with on PC, Web-Based PC and Tablet PC (PDA).

Doyle et al.[30], they compare the accuracy of observer performance Personal Computer (PC) compared with dedicated PACS workstation display in the detection of wrist fractures on computed radiographs. Seven observers independently assessed randomized digital radiographs of the wrist. And they used follow-up radiograph and/or computed tomographic scan as the reference standard.

McDonald et al.[31], they studied the accuracy of interpretation of diagnostic images among users of PACS diagnostic workstation, compared with a less costly Web-Based imaging system on a personal computer (PC) with a high resolution monitor. One hundred pediatric chest or abdomen and skeletal X-ray were selected two senior radiologist viewed and rated each image and after that the data were coded as correct or incorrect in accordance with the reference (the radiologists' classification). McNemar test and Ninety-five percent confidence interval (CIs) were calculated as Statistical Analysis.

Lee et al.[32], They have assessed the observer performance of urolithiasis detection on a tablet PC (PDA) and compared these results to the detection sensitivity using traditional soft-copy reading at PACS workstation. A total eighty computed radiography (CRs) obtained from the 80 patients were evaluated the result of the intravenous urography (IVU) study and clinical records were used as the gold standard to determine the presence of renal or ureteral stones. Two radiologists were blind to the information and result of IVU review each image. This study provides evidence for the use of Tablet PCs as a mobile PACS.

Therefore, PACS directly related to DICOM. Their functionality work is driven to make them work together. This is why the equipment or software with self-PACS DICOM compliant. Each vendor has the Conformance Statement for DICOM as an individual document, which is a very important document explaining the extent to which the device supports the DICOM standard. In real meaning, PACS bring the DICOM standard to life.

In addition, DICOM is also applicable to an off-line media environment. The ACR-NEMA Standard did not specify a file format or choice of physical media or logical file system. DICOM supports operation in an offline media environment using industry standard media such as CD-R and MOD and logical file systems such as ISO 9660 and PC File System (FAT16).

DICOM has truly formed the landscape of modern medicine by providing:

a) High image quality. DICOM supports up to 65,536 (16 bit) shades of gray for monochrome display is super fine. In comparison to images conversion DICOM into JPEGs or bitmaps (BMP) that was limited to 256 shades of gray

b) Wide support. DICOM fully supports all parameters and data type. Not only store the images but also record many of the other parameters involved, such as patient positioning 3-D physical size of objects in the picture, the thick piece of the exposure to images, and other useful data.

c) Absolute information encoding. DICOM contained thousand standardized attributes (DICOM data dictionary) to express various medical data. This information is needed for accurate diagnosis and to capture all aspects of radiation.

d) Standard of digital medicine format. All image acquisition devices currently provide DICOM and all communication over the network support DICOM. Current medical workflow is controlled by DICOM.

3.4.1. Basic DICOM File Structure

A DICOM file is easily divided into two main parts which are the DICOM image and the data header**.**

An illustration of the basic file structure can be seen table 3.1.

Table 3.1 Structure of DICOM file

Preamble	First 127 byte contain called preamble.
Prefix	.dcm or .dicm is the prefix
Data Element	All related data values are stored here.
Data Element	
.	.
.	
Data Element	.
Image	Stored the Pixel Density

A DICOM file contains binary *attribute* or data elements. Each element consists of A tag, in the format of group, element (XXXX,XXXX) that identifies the element. A Group Number tells you about an entity. An element number identifies the exact information in the group.

For Example, In the tag (0010,0020): Group No. is 0010 and Element No. is 0020. The Group no. 0010 tells you that the information is about PATIENT and the Element No. 0020 tells you that the information is about the PATIENT NAME.

Some Groups: (Group numbers are in Hexadecimal)

Group 2: Contains File Meta information

Group 8: General series info.

Group 10: Patient info.

Group 20: General Study info.

Group 28: Image info. Etc.

A Value Representation (VR) describes the data type and format of the attribute's value. It is an optional field. A value length (VL) defines the length of the attribute's value. A value field is containing the attribute's data. Each data element must be read in order to march through the file and find the data of interest.

The current DICOM standard specifies that the file contains the string "DICM" starting at byte position 128.

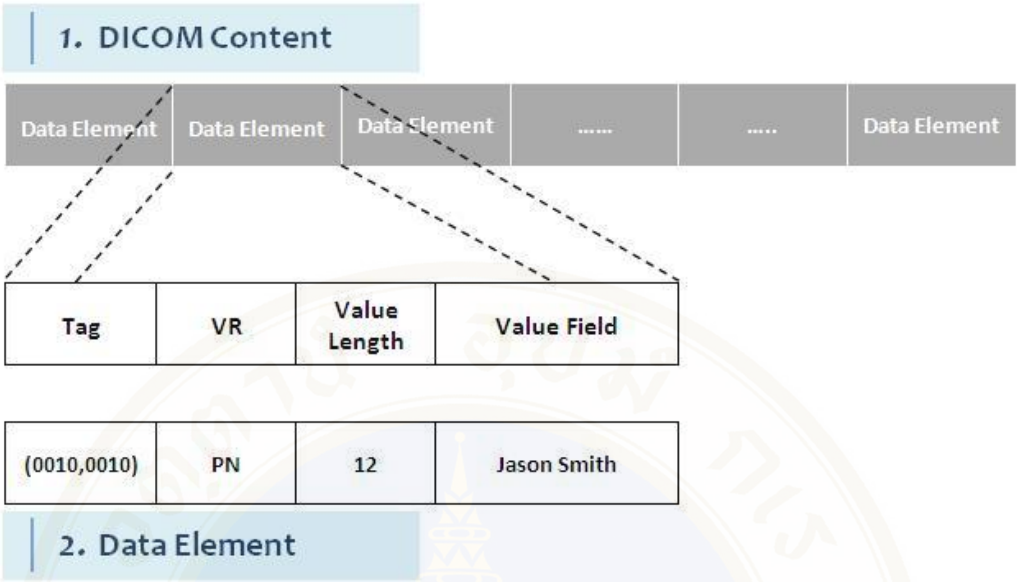

Figure 3.16 The data elements consisting of TAG, VR, Value Length and Value field.

Each data element is described by a pair of numbers (group number, data element number). Even numbered groups are elements defined by the DICOM standard and are referred to as public tags. Odd numbered groups can be defined by users of the file format, but must conform to the same structure as standard elements. These are referred to as private tags.

There are dozens of companies, such as Siemens Healthcare, GE Healthcare, and Philips Healthcare etc. which market the instrument that are universally compatible with most imaging systems. Each vendor often customizes the specific software for operation coupled with the instrument. [7,33]

DICOM files from different devices have specific information, in this research we used the DICOM file from PET.

So we will give you an idea about examples of the relevant information from PET DICOM file in the next section.

3.4.2. PET Information Object Definition

The Positron Emission Tomography (PET) Image Information Object Definition specifies an image which has been created by a positron tomograph imaging device, including dedicated PET cameras and Nuclear Medicine imaging devices operating in coincidence mode. This includes data created by external

detection devices which create images of the distribution of administered radioactive materials, specifically positron emitters, in the body.

Depending on the specific radiopharmaceuticals administered and the particular imaging procedure performed, problems involving changes in metabolism function, or physiology can be investigated and various region pathologies can be studied. For these problems, quantitation of image data in absolute activity and physiological units is important. In addition, the PET Image IOD specifies attenuation (transmission) images used for correction and anatomical reference of emission images. [4]

In PET DICOM file that enclose images and the series of data . These Modules contain Attributes that are specific to Positron Emission Tomography images.

DICOM file contains IOD Attributes that describe all about PET such as

- *PET Series* included attributes Series Date, Series Time, Units, Counts Source, Series Type, Reprojection Method, Number of Time Slices, Number of Slices,Corrected Image, Randoms Correction Method, Attenuation Correction Method, Scatter Correction Method, Decay Correction, Reconstruction Diameter, Convolution Kernel, Reconstruction Method, Detector Lines of Response Used, Acquisition Start Condition etc.

- *PET Isotope* included attributes Radiopharmaceutical Information Sequence, Administration Route Code Sequence, Code Value, Radiopharmaceutical Volume, Radiopharmaceutical Start Time, Radiopharmaceutical Stop Time, Radionuclide Total Dose, Radionuclide Half Life, Radionuclide Positron Fraction, Radiopharmaceutical Specific Activity etc.

- *PET Multi-gated Acquisition* included attributes Beat Rejection Flag, Trigger Source or Type, PVC Rejection, Skip Beats, Heart Rate, Framing Type

- *PET images* included attributes Image Type, Samples per Pixel, Bits Allocated, Bits Stored, High Bit, Rescale Intercept, Rescale Slope, Frame Reference Time, Trigger Time, Frame Time, Low R-R Value, High R-R Value, Lossy Image Compression, Image Index, Acquisition Date, Acquisition Time, Actual Frame Duration, Nominal Interval, Intervals Acquired, Intervals Rejected, Primary (Prompts) Counts Accumulated, Secondary Counts Accumulated, Slice Sensitivity Factor etc.

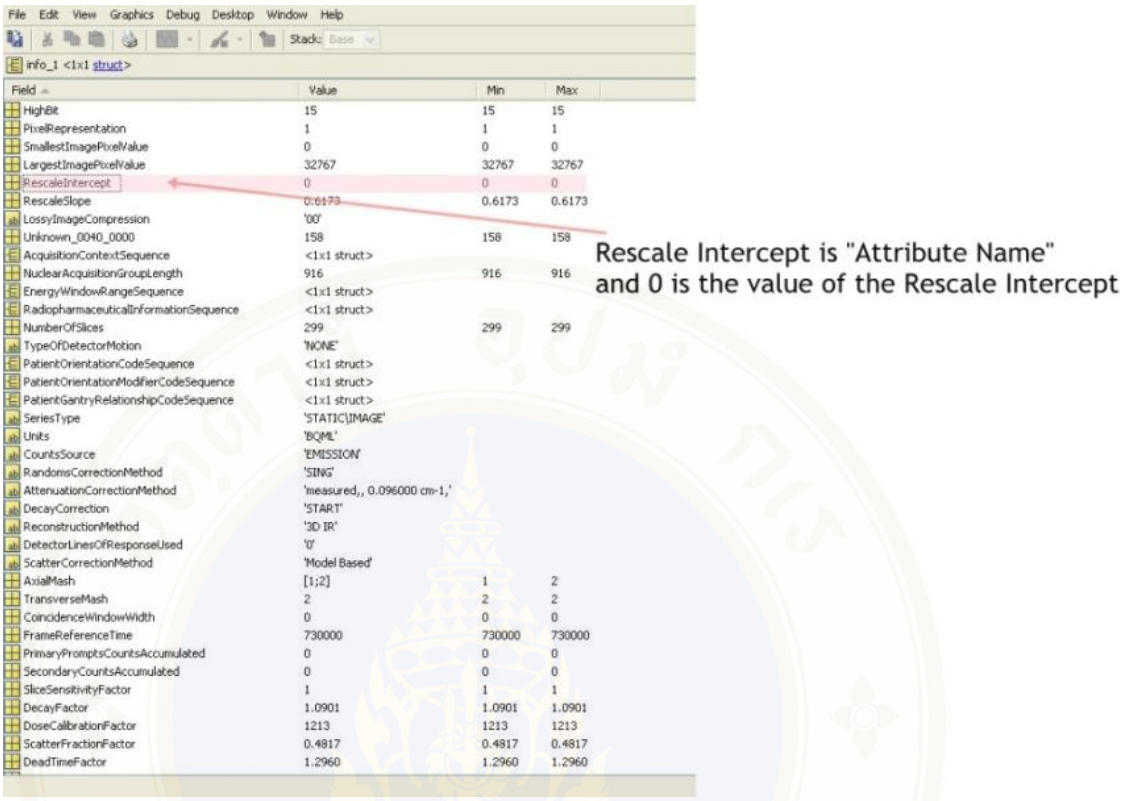

Figure 3.17 DICOM header viewed from MATLAB

From the Fig.3.17, the DICOM conformance[4] gives more detailed explanation about the Rescale Intercept attribute as in table 3.2.

Table 3.2 Example Attribute in the conformance.[4]

Attribute Name	*Tag*	*type*	*Attribute Description*
Rescale Intercept	(0028,1052)		The value b in relationship between stored values (SV) and pixel value units (U) defined in Units (0054,1001): U = m*SV+b. The Rescale Intercept is always zero for PET images.

And every Attribute can be found the further meaning from the conformance as well.

In our research, we analyze the SUV from DICOM files. The first step is understanding in the relevance and relation of SUV and DICOM file, which has many steps and several parameters involved. The relevant references are in the following

Kanakatte et at[6], They present a novel segmentation scheme for detection the tumor alone in lung PET images using standard uptake value (SUV) and connected component analysis and also compare this scheme with several commonly used medical image segmentation techniques like threshold, Sobel edge detector, etc.

Discovery STE from GE has been used as a PET/CT tool in this study. Information [3,34] meaning of DICOM TAG and Procedure for computing SUV are obtained from the GE Document. [5,35,36]

This chapter is a gathering of meaning and theories associated to the research, including Basic physics and instrumentation of PET, Radiopharmaceutical, Standardized Uptake Value (SUV), DICOM, and including some literature review in the end of each topic.

CHAPTER IV
MATERIALS & METHODS

Since the similar study is not much prevalent. So We have to start doing the research by PILOT STUDY. The purpose of pilot study is for studying the characteristic of DICOM file type, that would be used in the research. The Pilot study has done by scanning phantom instead of patients. Then the obtained files could be used for study further.

The purpose of the Pilot Study shows by the following chart

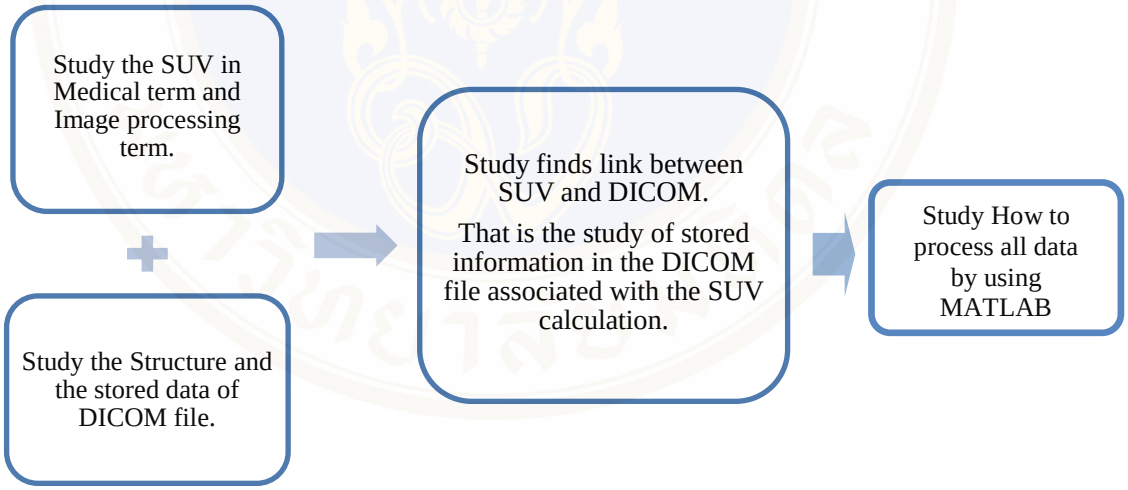

Figure 4.1 Chart of the step of study

4.1. MATERIALS

4.1.1. Radiopharmaceutical

- [^{18}F] Fluro-2-deoxy-D-Glucose (^{18}F-FDG)

4.1.2. Equipment Description

- General Electric Discovery STE®

- WCC Phantom
- DICOM PET-CT files

4.1.3. Program Application

- Xeleris® Functional Imaging Workstation for PET/CT
- MATLAB
- SPSS (Statistical Analysis)
- Microsoft Excel 2007

4.2. MATHODS

4.2.1. Pilot Study

In this study, we used DICOM files from Phantom scan (PILOT STUDY). It must be prepared, and we use the WCC phantom or well Counter Correction Phantom and do the scan according to the Phantom preparing for Quarterly QC. [35]

Preparing & Scanning WCC phantom

(a) Adjust a holder with columnar WCC phantom before putting Activity into here.

(b) After this, work will be done in the Laboratory or else like

(c) Remove water inside phantom a little and put in 18F-FDG of well-known amount of radioactivity. Put the time of Dose calibrator which measures the amount of radioactivity at this time, and the PET/CT scanner itself together

(d) Stir the water inside phantom with being careful that a bubble doing not appear. (be careful not to spill a liquid as much as possible)

(e) Fill phantom with the water and being careful that a bubble becoming a minimum.

(f) Carry out it from the room, and set on a holder of the scanner with being careful of the pollution.

(g) Scan WCC phantom with the same protocol as with patient.

(h) After the scan, we get a set of DICOM files. We used files that have already been corrected by the attenuation correction.

Figure 4.2 Picture of WCC Phantom

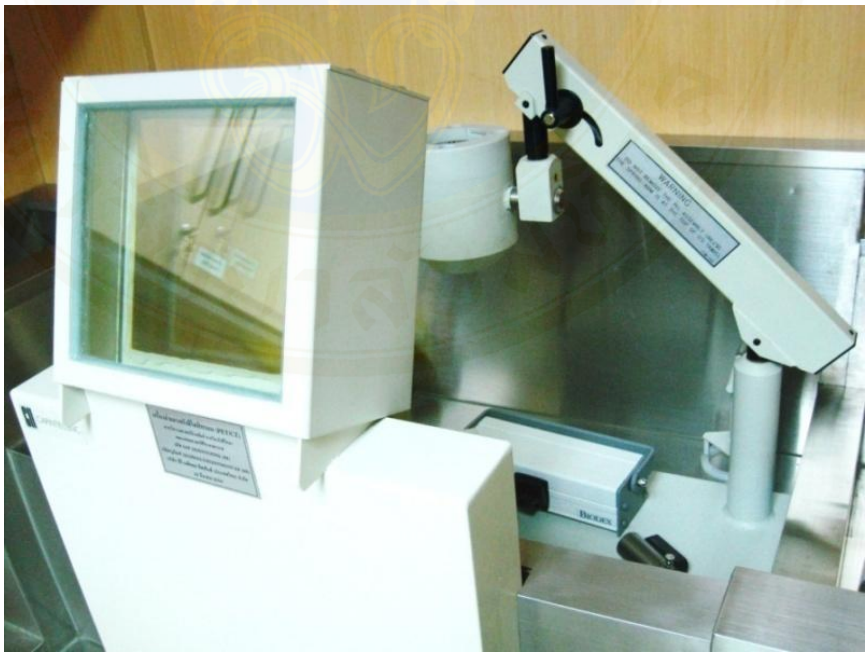

Figure 4.3 The working area of the Radiopharmaceutical Preparation with shielding.

4.2.2. Study Framework

A block diagram shown (Fig. 4.4) is the entire process of our SUV calculation scheme. After a set of DICOM files passed through our created scheme, the SUV are yielded.

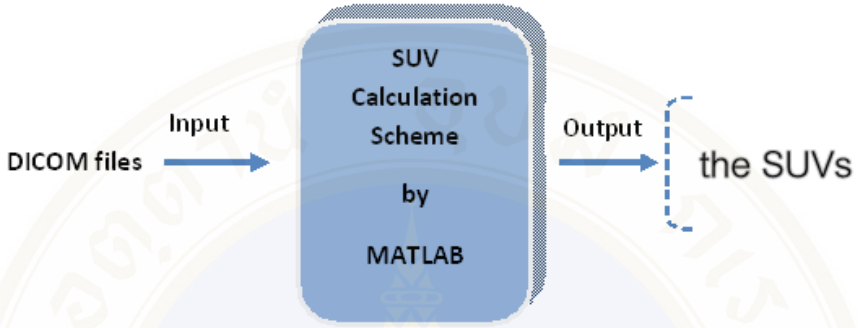

Figure 4.4 The Study Framework

4.2.3. Calculation of Standardized Uptake Value (SUV)

SUV (Standardized Uptake Value) is the value that quite often used. It is most commonly used semi-quantitative parameter utilized for analyzing FDG-PET images in routine clinical practice. It came to be used as a tool to supplement visual interpretation. The SUV is also used to distinguish between malignant and benign tumor.

In this study, the DICOM files are the main source to analyze and calculate SUV. The Component of the DICOM file can be divided into 2 main parts which are the image and metadata. The image is the part that displays the information by image and the metadata is the part that keeps the detail of the data such as dose of injection, type of scan, patient weight, patient name, etc.

We calculate the Standardized Uptake Value (SUV) and the brief meaning of SUV is the Differential Uptake Value, Dose Uptake Ratio, or Dose Absorption Ratio. For this study we used PET DICOM file that has been through the attenuation correction.

The Uptake Value is represented by Pixel intensity value in the image and the GE DICOM file. It collects the data in 16 bits so that the pixel intensity value is between 0-32767.

Therefore, the first process of the SUV calculation is the conversion of the pixel intensity value in a region of interest (ROI) to the activity concentration.

Either $SUV_{maximum}$ or SUV_{mean} in a region of interest (ROI) can be used. Nevertheless physician prefers to report the case by the Maximum SUV. Because the maximum SUV is least affect by partial volume effect[15], so in this research we calculate the SUV_{max} which is obtained from the Maximum Pixel Value in the image slice.

The related attributed tag for the conversion is Rescale Slope tag, and Rescale Intercept tag (there are from metadata part). These tags vary for each image slice. So the tissue activity is calculated by

$$U = m \bullet SV + b \qquad \ldots(4.1)$$

Where *m* is rescale Slope (which is different in each image slice), *SV* is the stored value (Pixel intensity Value), *b* is rescale intercept (for PET scan is always Zero) and *U* is units of value after conversion (for our study is *Bq/ml*, Shown in Unit tag)

The conversion formula above is fundamentally defined by NEMA, however the formula maybe slightly different for each vendor. In this study we used GE DICOM file. So the method of calculation is based on GE conformance statement [9]

$$SUV_{body\ weight(kg/ml)} = \frac{Activity\ Concentration\ in\ ROI_{(Bq/ml)}}{\left(\frac{Injected\ Dose_{(Bq)}}{body\ weight_{(kg)}}\right)} \qquad \ldots(4.2)$$

$$SUV_{body\ weight(kg/ml)} = \frac{\left(Pixel\ Value \times \text{Im}age\ \text{Re}scale\ factor \times dose\ calibration\right)}{\left(\frac{actual\ activity}{body\ weight}\right)} \qquad \ldots(4.3)$$

Where *Pixel Value* is Pixel Intensity Value in Region of Interest (ROI), Image Scale Factor = Rescale Slope, , *Actual activity* is Injected activity at the time of scan, *Body*

weight is Patient Body Weight *(kg)* and *Dose Calibration factor* must be corrected for *MBq/ml* to *Bq/ml* conversion.

In the process of SUV calculation. Image and metadata are both required. So, an application program is needed and in this research, It was MATLAB because MATLAB supported for DICOM file.

The SUV formula (4.2) requires data from both image part and metadata part so we used MATLAB to extract these data.

The steps of the SUV calculation scheme are summarized as follows:

Step 1: Extract Pixel Intensity Value in Defined ROI (region of interest).

The purpose of extraction is to note the obtained pixel intensity value for the next step of calculation, so we extract Maximum pixel intensity because we need them to calculate the SUV_{max}

Step 2: Convert Intensity Pixel Value to activity concentration (Bq).

After we extracted the desired value, the conversion of Intensity Pixel Value to Activity Concentration (Bq) is the next step. The data in this conversion based on some of the detail part (metadata). See formula (4.2) then become

$$\text{Activity Conc. in ROI}_{(\text{Bq/ml})} = \text{Pixel Value} \times \text{Image Scale Factor} \times \text{dose calibration} \quad \ldots(4.4)$$

$$\text{Image Scale Factor} = \text{Rescale Slope} \quad \ldots(4.5)$$

Where The related tags in this part are Rescale Slope, Rescale Intercept, dose calibration and Units. Only Rescale slope is individual in each slice.

Step 3: Calculate SUV in each slice.

Calculate SUV by formula (4.3) which the related tag in this part are Total Dose (0018,1074), Series Date (0008,0021), Series Time (0008,0031), Radiopharmaceutical Start Time (0018,1072), Radiopharmaceutical Half Life (0018,1075) andPatient Weight (0010,1010)

Step 4: Integral SUV of ROI to VOI

In practical, SUV calculation is analyzed in the Volume of Interest (VOI). So In this study we calculated SUV in each slice and then summarized

them which is depending on number of slices and projected the region of interest into every slice in the volume. Mean that every slice under the volume has the same size and position.

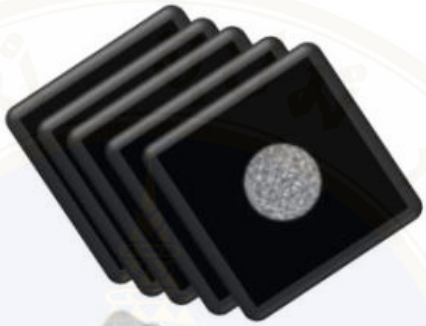

Figure 4.5 Integral regions to volume (ROIs to VOI)

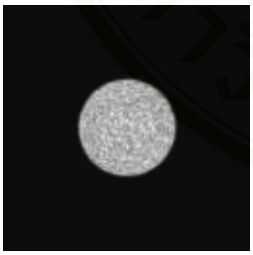

Field	Value	Min	Max
PixelDataGroupLength	32780	32780	32780
ImageIndex	83	83	83
DeadTimeFactor	1.0365	1.0365	1.0365
ScatterFractionFactor	0.2066	0.2066	0.2066
DoseCalibrationFactor	1213	1213	1213
DecayFactor	1.0291	1.0291	1.0291
SliceSensitivityFactor	1	1	1
SecondaryCountsAccumulated	0	0	0
PrimaryPromptsCountsAccumulated	0	0	0
FrameReferenceTime	183000	183000	183000
CoincidenceWindowWidth	0	0	0
TransverseMash	2	2	2
AxialMash	[1;2]	1	2
ScatterCorrectionMethod	'Model Based'		
DetectorLinesOfResponseUsed	'0'		
ReconstructionMethod	'3D IR'		
DecayCorrection	'START'		
AttenuationCorrectionMethod	'measured,, 0.096000 cm-1,'		
RandomsCorrectionMethod	'SING'		
CountsSource	'EMISSION'		
Units	'BQML'		
SeriesType	'STATIC\IMAGE'		
PatientGantryRelationshipCodeSequence	*<1x1 struct>*		

(a) (b)

Figure 4.6 The DICOM file is reviewed by MATLAB (a.) Image part (b.)Header (Metadata) part.

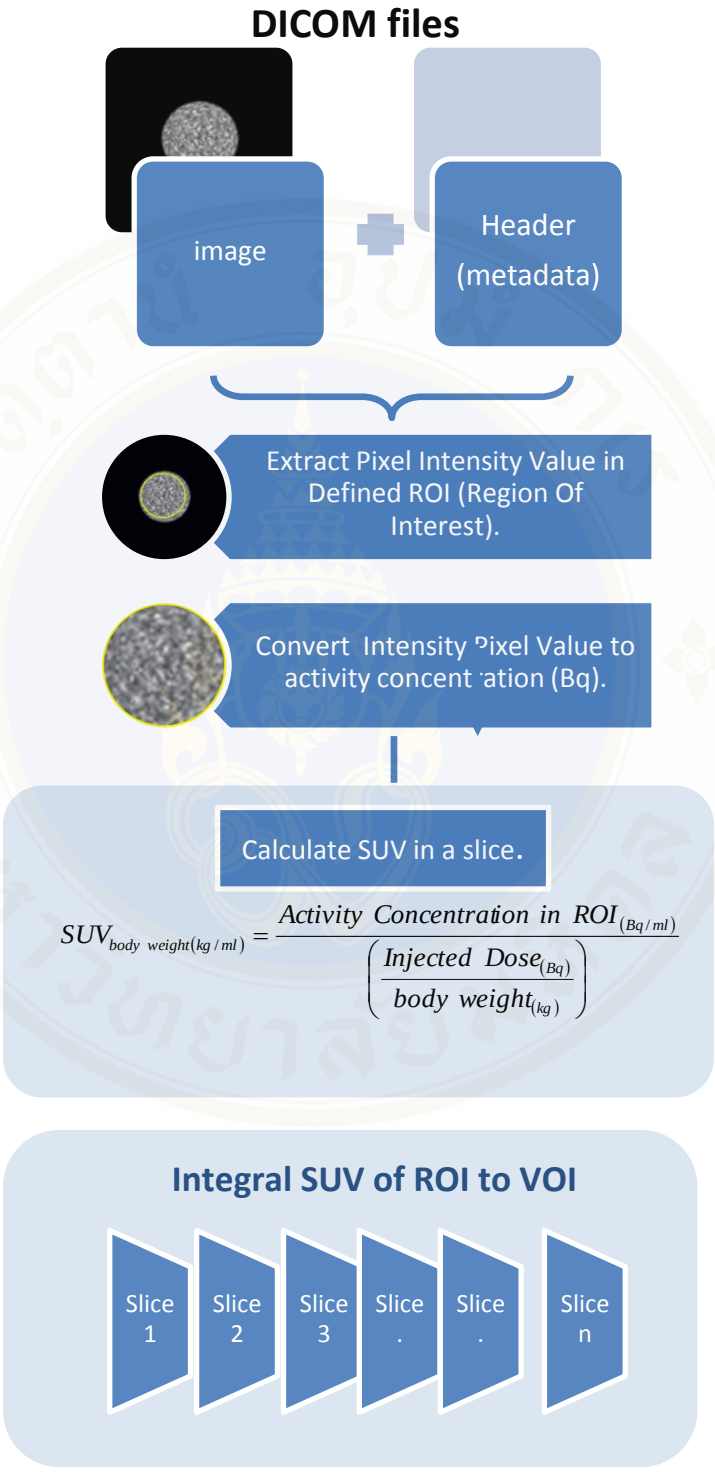

Figure 4.7 calculation of SUV in our new scheme term

4.2.4. Data Collection & Analysis

For more practicable the SUV calculation Scheme testing is needed. This research will use the same sample to compare SUV from two methods. This SUV calculation Scheme is operated on the PC with installing MATLAB. In order to evaluate the performance of the scheme, it is compared to the SUV that obtained from the Well-known application software from GE healthcare (Xeleris workstation).

The scheme will be tested by inputting the PET DICOM file. The first aspect in this comparison is both system need to proceed in the same file. After a study of GE healthcare DICOM file by doing the PILOT STUDY, we found that GE healthcare has stored the DICOM file by arranged inversely. The first file (Slice No.1) on Xeleris is the last DICOM file (Slice No.277) on MATLAB.

Both Xeleris and MATLAB (the SUV calculation scheme) allow interpretation of ROI analysis. The circular ROIs were drawn surrounding the region of FDG uptake (lesion). In each patient consisted many of file slices according to each lesion on each patient. The SUV in the defined region was recorded by the Xeleris® workstation and MATLAB.

The main SUV calculation scheme was created as an application that can calculate the SUV by drawing immediately on the DICOM files that you want to know. Both systems needed to analyze on the same file, and also matched region of interest (ROI). The ROI within slice was drawn in the same location and size. So that the another application needed to be created to compare them both. It was run by calling the file as ROIs model (include position and shape) for the next DICOM file to compare.

The briefly step of the data collection and the application's running would be shown on the following.

*Procedure on **Xeleris Workstation***

1. View the SUV values on Xeleris workstation.
2. Recorded the Slice Number and the SUV_{max}.
3. Capture screen of images with ROI. It used as the model file to determine on the next MATLAB. In this research, the ROI was drawn in 2.5 cm diameter by size through all slices.

4. For the patient file. we discovered the interested lesion in a set of slice which cover all the lesion, and draw the same ROI size within same location through all slices in the set. All ROIs was drawn on the image with a cross-section (transaxial) view. (On the Xeleris workstation, we can set screen to show the location of the ROI, so be attention that all slices in a set located in same position.)

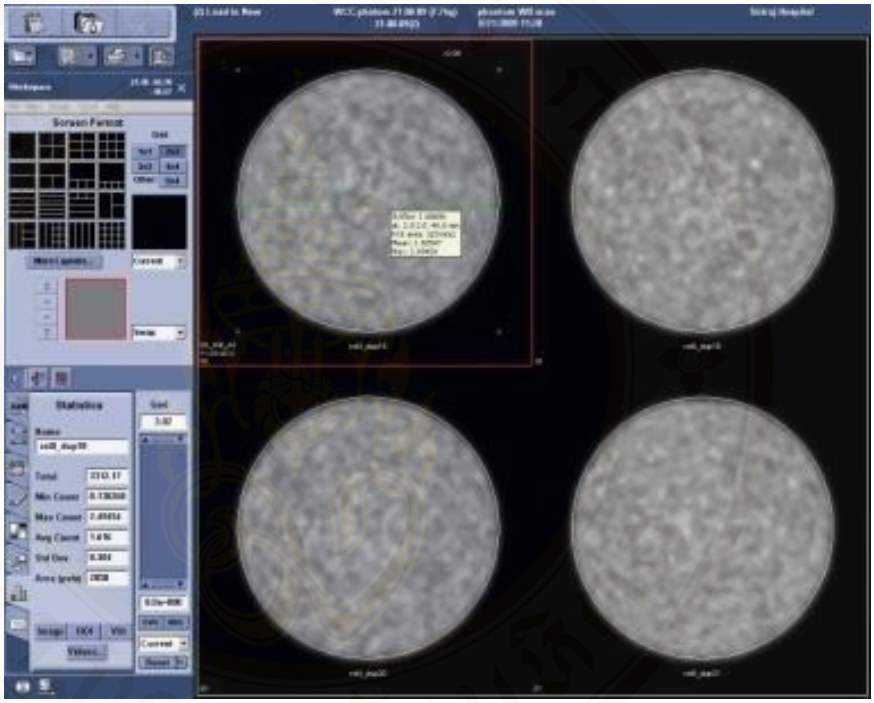

Figure 4.8 The screen of Xeleris Workstation from GE healthcare.

*Procedure on **MATLAB.***

1. Run: >> suvdicom , the SUV calculation scheme we created. ("suvdicom" is the name)
2. Browse a jpg file that we use as ROI model to a DICOM file in the next step.

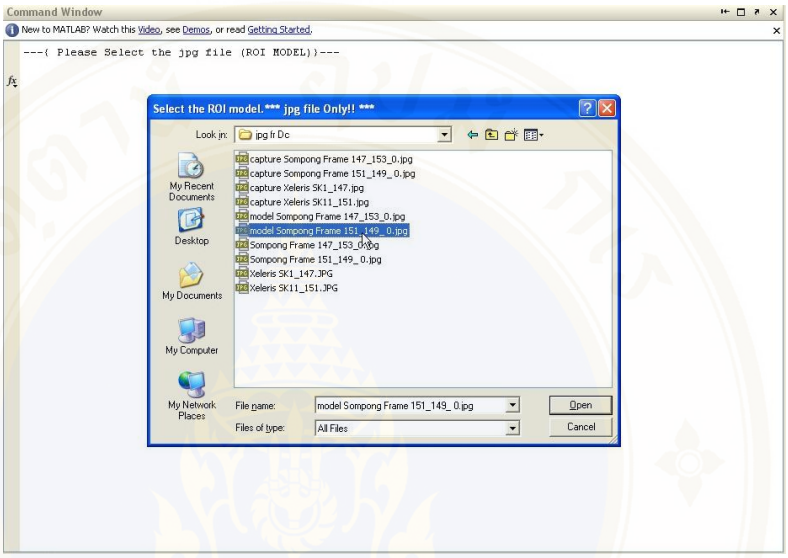

Figure 4.9 MATLAB screen window showed the step of browsing model files.

3. Draw a ROI over the boundaries of ROI that appear on the jpg file and then press Enter.

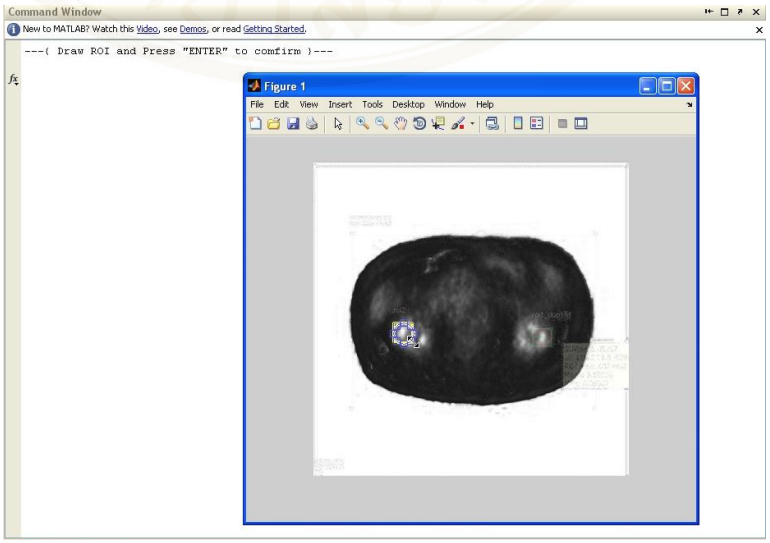

Figure 4.10 MATLAB screen window showed the step of ROI drawing

4. After all, the program will ask for a DICOM file, so browse for select DICOM file (can select more than one file). It will calculate a position above on the selected DICOM file. Be attention that the Number of DICOM file must be associated with the ROI model.

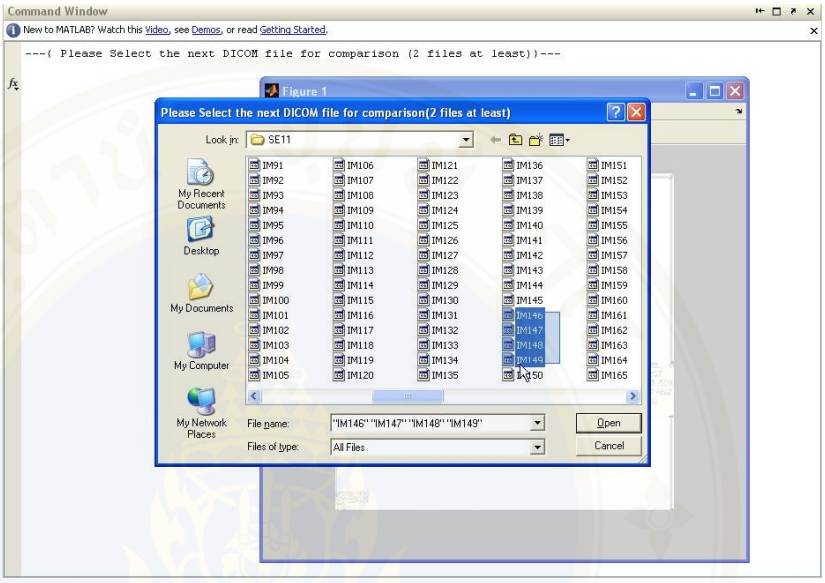

Figure 4.12 MATLAB screen window showed the step of browsing DICOM files

5. The Output was shown.

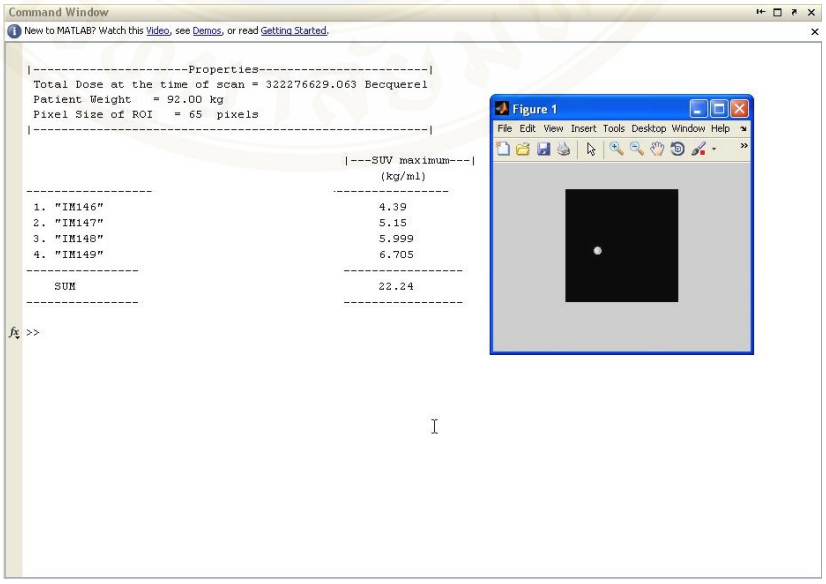

Figure 4.13 MATLAB screen window showed the output.

6. Record the SUV from Xeleris and MATLAB in the following table.

Table 4.1 The data table for recording SUV from the slices.

	Image No.	SUVmax (kg/ml)		
		Xeleris	MATLAB	
Patient 1 , Series 1	IM 9			Total Dose = Bq. PtWeight = kg. ROI Pixel Size = pixels.
	IM 10			
	IM 11			
	.			
	.			
	.			
	SUM			

Table 4.2 The data table for recording the summarized SUV from 11 patients.

Sample	SUV(kg/ml)		% Difference
	Xeleris	MATLAB	
1			
2			
3			
.			
.			
11			
SUM			

The statistical analysis was tested using SPSS version 11.5 and Microsoft excel. The correlation between two variables reflects the degree to which the variables are related. The most common measure of correlation is Pearson's Correlation. Pearson's correlation reflects the degree of linear relationship between two variables. It is used when both variables are at least at interval level and data parametric.

The SUV from new MATLAB scheme was compared to the Xeleris workstation. It was performed with 108 file slices from 11 patients. The correlation of both systems was analyzed with Pearson's correlation technique. The accuracy of new scheme was tested by calculated the relative error between both system and distribution of these result were tested.

Summary of the sampling procedure and data analyses was shown in Fig. 4.14.

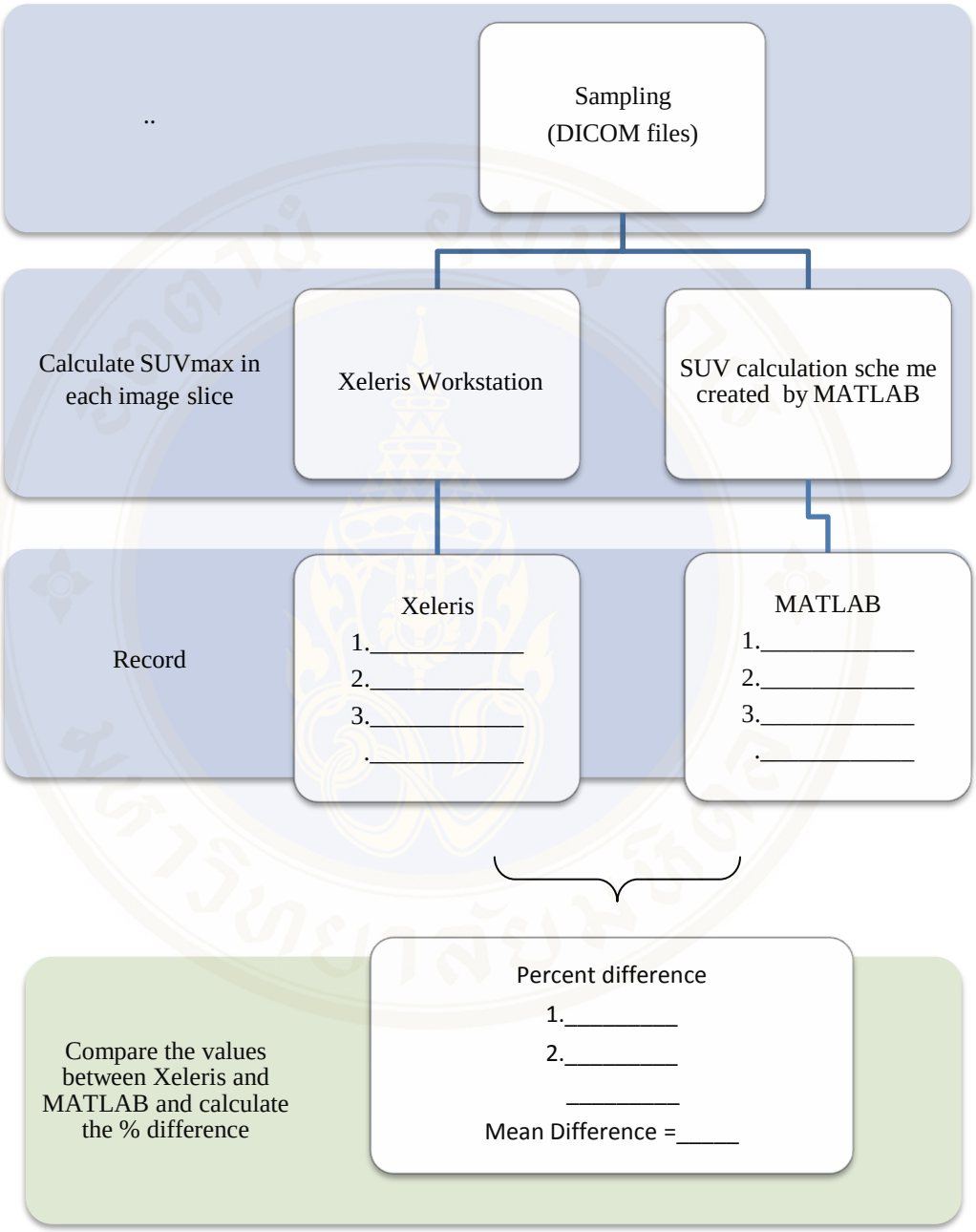

Figure 4.14 Summary steps in procedure of sampling and data analysis

In this chapter, the involved materials, equipment and methods that divided into 3 major steps were shown.

1. Pilot Study, which outlines the steps of DICOM file preparation by using the phantom scan.

2. SUV calculation, provided the detail of new SUV calculation scheme created by MATLAB.

3. Data collection and Analysis, detailed the data collection on Xeleris workstation and running SUV calculation scheme on MATLAB, including a comparative study between both methods.

CHAPTER V
RESULTS

The SUVs from the new scheme which was created by MATLAB were directly compared with the well known PET/CT application, Xeleris Workstation.

It was performed the comparison by using 108 slices of DICOM files that were obtained from 11 patients (8 men, 3 women). Those files were randomly sampled by computer. They were taken through F18-FDG PET/CT scanning at Siriraj Imaging Center during January to October 2010.(see appendix)

5.1. Correlations of Two Methods

SPSS version 11.5 and Excel were used as a tool for the statistical analysis. The basic descriptive statistic was shown as the mean, the standard deviation, and the standard error of mean of data that computed from both Xeleris workstation and was created from MATLAB (Table 5.1).

Table 5.1 Basic statistical description of 108 SUVs from the Xeleris workstation and MATLAB scheme.

	N	Mean	Std. Deviation	Std. Error Mean
Xeleris	108	12.0172	6.54119	.62943
MATLAB	108	10.3835	5.43024	.52253

The SUV from Xeleris Workstation and MATLAB were compared by the Pearson correlation Test.

Table 5.2 The correlation of maximum SUV between 2 systems.

Correlations

		Xeleris	MATLAB
Xeleris	Pearson Correlation	1	.974(**)
	Sig. (2-tailed)	.	.000
	N	108	108
MATLAB	Pearson Correlation	.974(**)	1
	Sig. (2-tailed)	.000	.
	N	108	108

** Correlation is significant at the 0.01 level (2-tailed).

Table 5.2 showed high correlation coefficient of 0.974 indicating a close correlation of results from Xeleris workstation and MATLAB. R^2 is 0.9487, we can say that about 99% of comparable capability to predict the SUV_{MATLAB} from $SUV_{Xeleris}$, 1% remain for other factors plus randomness.

5.2. Accuracy of the MATLAB Scheme

The performance of MATLAB scheme was tested by comparing the obtained SUV_{max} to the Xeleris Workstation. In addition to the correlation test, the accuracy calculation is also used. The accuracy of MATLAB scheme was indicated by the relative error which can be calculated by

$$RelativeError = \frac{|SUV_{Xeleris} - SUV_{MATLAB}|}{SUV_{Xeleris}} \times 100 \quad \ldots(5.1)$$

$$\%Accuracy = 100 - RelativeError \quad \ldots(5.2)$$

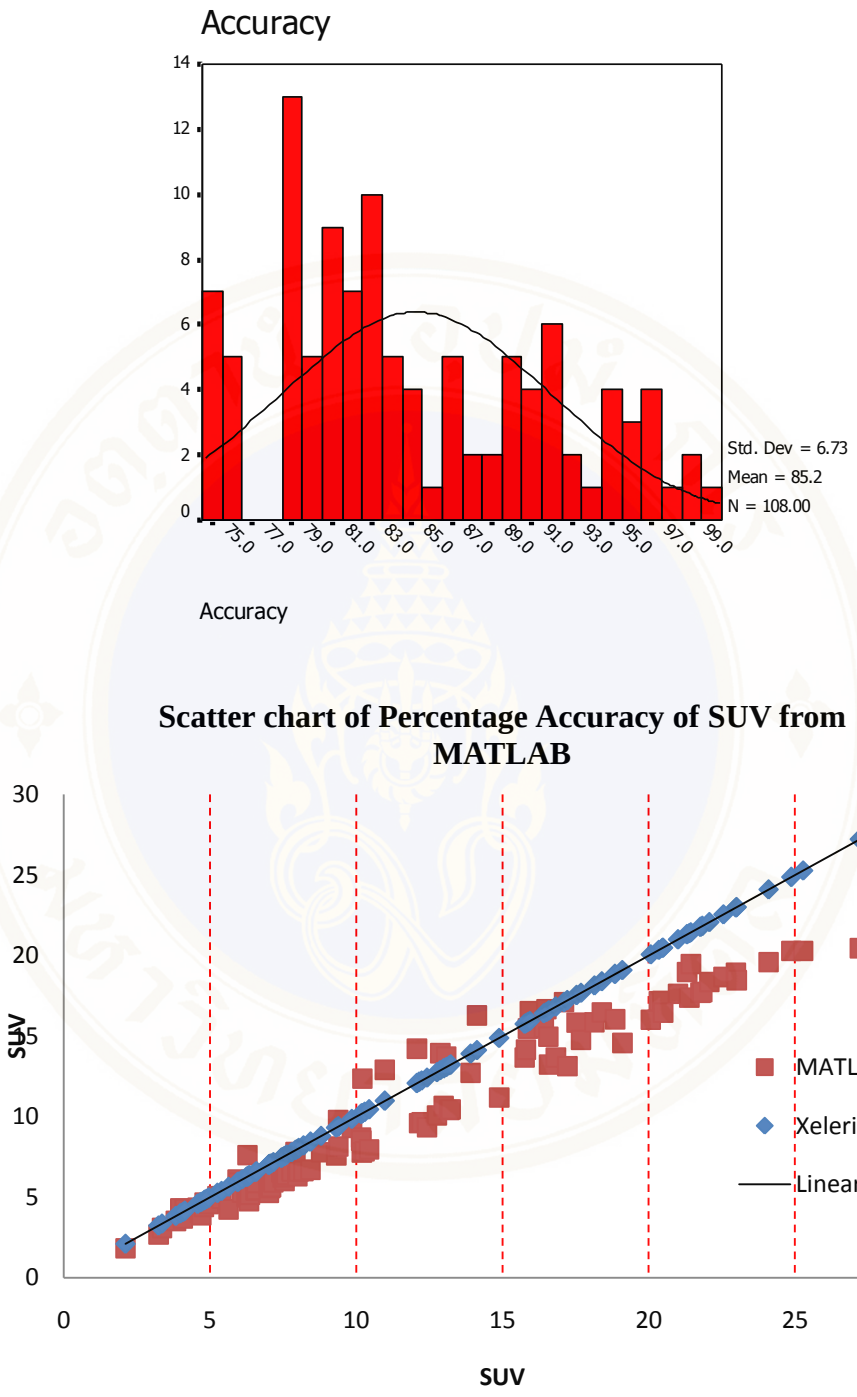

Figure 5.1 Histogram and Chart of the percentage accuracy from MATLAB and Xeleris workstation.

The output from basic statistical testing by SPSS showed the Skewness and Kurtosis. These values can be used to assess the distribution of data.

The Skewness and Kurtosis statistic value are 0.462 and -0.835 the standard error of them are 0.233 and 0.461. It is useful for figuring out the dispersion and the distribution of data. So we calculate at the 95% confidence interval by

$$Skewness = StatisticValue_{skewness} \pm 1.96(Std.Error_{skewness})$$

0.5320 ●——————● 0.9186

$$Kurtosis = StatisticValue_{Kurtosis} \pm 1.96(Std.Error_{Kurtosis})$$

-1.7385 ●——————● 0.0685

Within the range of both skewness and kurtosis are "0" (zero), it means that the percentage accuracy of MATLAB is normally distributed significantly with a 95% confidence interval.

Table 5.3 Statistical an analysis of accuracy of SUVs obtained from MATLAB scheme.

			% Accuracy	*Std. Deviation*	*Std. Mean Err.*
11 Patients N=108	**Mean**		**85.2036**	6.7329	0.6479
	95%Confidence Interval for Mean	Lower Bound	83.9193		
		Upper Bound	86.4880		
	- Minimum		75.16		
	- Maximum		99.96		

From table 5.3, the average of percentage accuracy is 85% and for the report at 95% confidence interval, the result ranged from 83.91% to 86.48%.

Table 5.4 The percentage accuracy of SUV arranges by range.

	% accuracy of SUV					
	X_a<5	**5<X_b<10**		**10<X_c<15**	**15<X_d<20**	**X_e>20**
1	86.54	96.46	82.62	85.5	86.82	79.8
2	82.64	90.95	93.11	83.68	89.58	84.38
3	91.92	75.18	87.74	76.3	97.46	83.97
4	92	97.37	83	78.95	96.15	80.28
5	92.11	98.86	79.45	76.32	94.54	83.96
6	90.48	86.7	82.63	76.31	98.91	89.06
7	97.06	80.86	83.74	82.4	90.33	81.3
8	94.78	79.46	84.79	82.24	79.8	90.84
9	85.94	79.01	98.49	78.98	81.3	81.29
10	82.62	75.18	78.99	78.97	99.96	81.27
11	91.56	80.9	82.18	75.19	76.31	83.16
12	96.82	82.71	80.87	79	90.33	82.78
13	94.64	82.55	79.45	91.73	83.46	82.38
14	92.35	89.25	88.49	82.06	87.42	80.27
15		90.78	81.57	95.03	89.58	81.28
16		80.87	95.62	78.98	85.14	81.57
17		75.18	86.71	78.99	76.32	80.25
18		92.52	94.35	91.47		75.17
19		78.98		84.69		75.2
20		79.45		75.16		
$\bar{X}$	**90.82**	**85.52**		**82.50**	**87.83**	**81.84**
SD	4.71	6.42		6.19	7.84	4.21

From the percentage accuracy of SUV from MATLAB scheme arranged by range (table 5.4), the result shows high accuracy in the lower range (at SUV < 5).

The chart in Fig.5.2 shows the percentage accuracy of SUV sorted by range from 0-30.

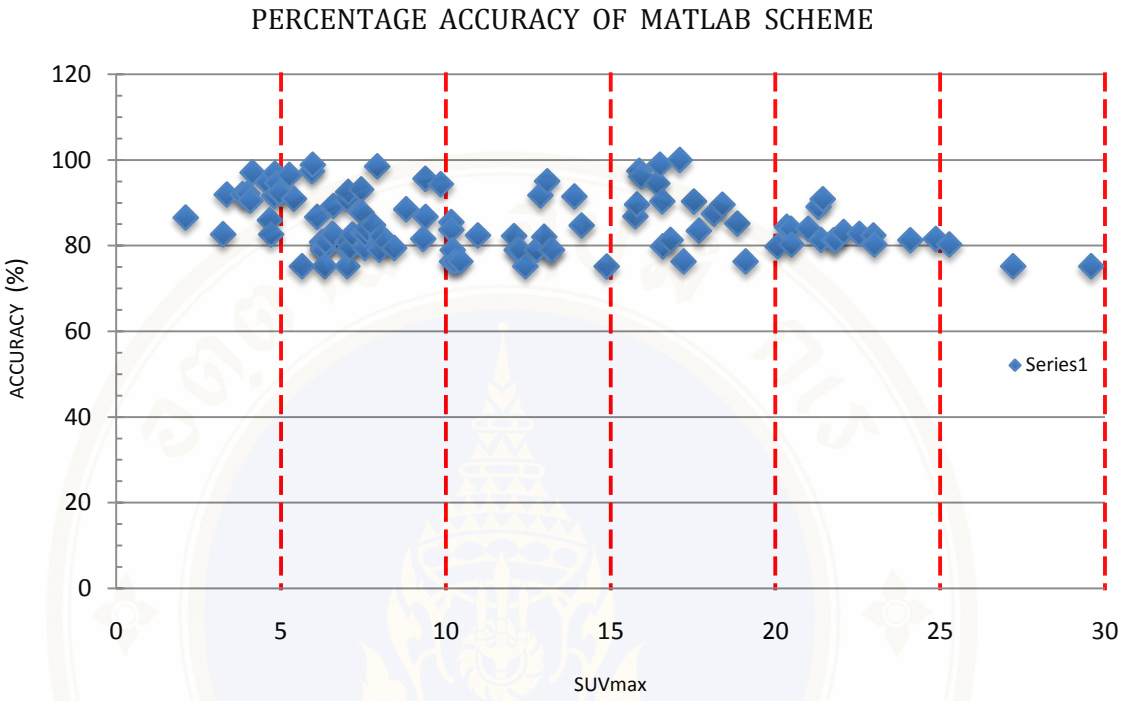

Figure 5.2 Scatter gram of percentage accuracy from the MATLAB scheme.

5.3. Individual Analysis

In addition, we also analyzed the SUV by individual patient. The graph and the statistical information are analyzed from 11 patients (see all raw data in the appendix).

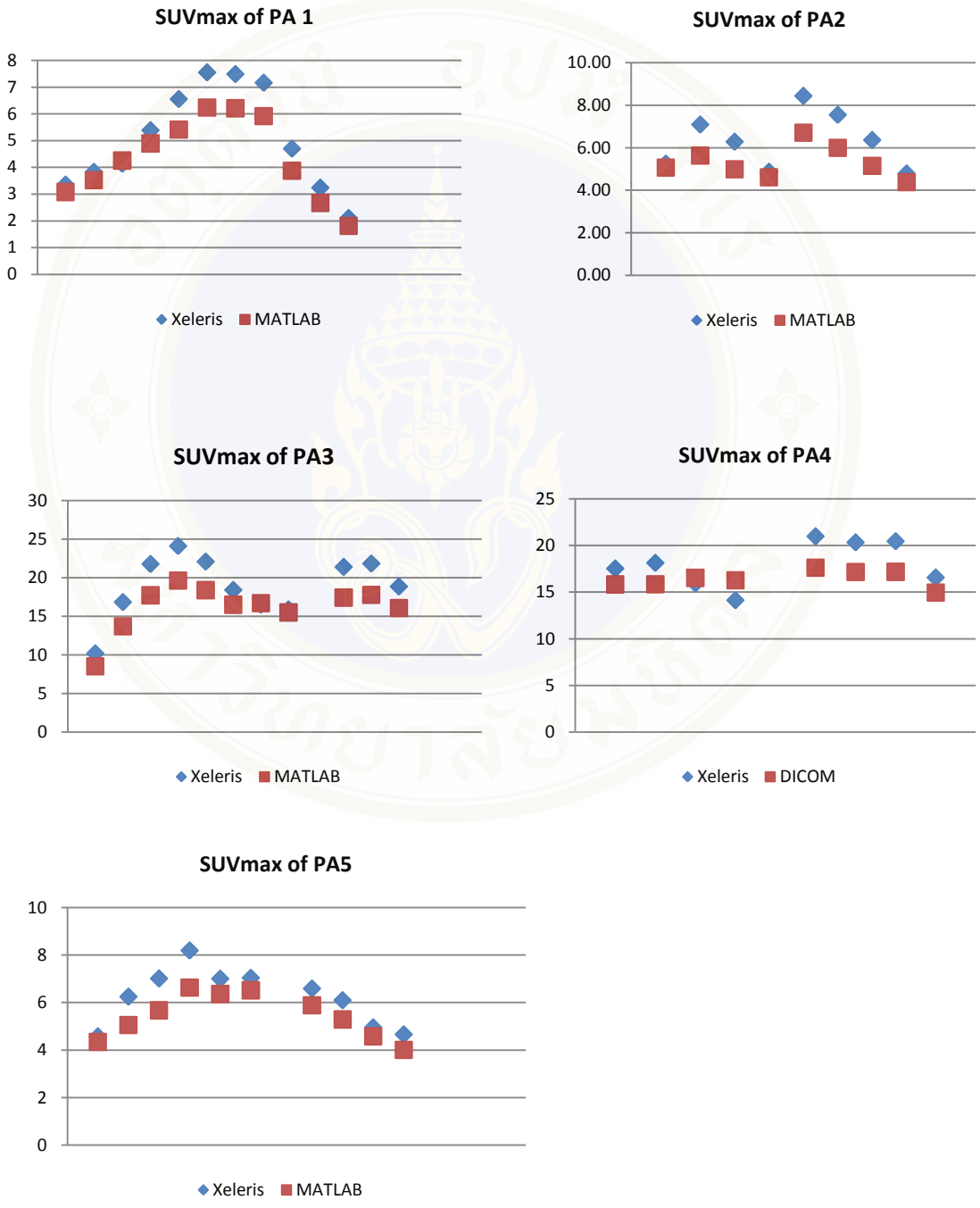

Figure 5.3 SUV_{max} distributions within each set of slices of patient 1 to patient 5.

Figure 5.4 SUV_{max} distributions within each set of slices of patient 6 to patient 11.

The SUV_{max} within slices in each patients.

In each patient, an average SUV varies according to the size of the tumor. This table shows the comparison of the SUV from Xeleris Workstation with the SUV scheme created from MATLAB

Table 5.5 Mean of the SUVs from a set of file slices shows in the individual term.

	N (slice)	Xeleris			MATLAB		
		Mean	Std. Deviation	Std. Error Mean	**Mean**	Std. Deviation	Std. Error Mean
PA1	10	**5.34**	1.7242	0.5452	**4.62**	1.3147	0.4157
PA2	8	**6.33**	1.3170	0.4656	**5.32**	0.7592	0.2684
PA3	11	**18.89**	3.9480	1.1904	**16.15**	2.9752	0.8971
PA4	8	**18.02**	2.4529	0.8672	**16.44**	0.8786	0.3106
PA5	10	**6.24**	1.1853	0.3748	**5.43**	0.9331	0.2951
PA6	13	**20.17**	3.7209	1.0320	**17.23**	2.6211	0.7270
PA7	12	**9.80**	2.8916	0.8347	**8.30**	1.8394	0.5310
PA8	9	**7.58**	2.4937	0.8312	**6.46**	1.7622	0.5874
PA9	8	**13.58**	3.7367	1.3211	**13.50**	1.9475	0.6885
PA10	10	**17.13**	13.877	4.3885	**13.51**	10.210	3.228
PA11	9	**10.84**	4.4382	1.4794	**9.06**	2.7938	0.9313

Table 5.6 Mean, minimum and maximum of percentage accuracy of the MATLAB scheme from each patient.

	Accuracy (%)		
	Mean	min	max
PA1	**86.79**	82.62	97.06
PA2	**85.17**	79.45	96.46
PA3	**85.55**	81.26	98.91
PA4	**87.66**	83.95	96.17
PA5	**87.40**	80.77	94.76
PA6	**85.89**	80.26	99.94
PA7	**89.53**	78.92	98.83
PA8	**84.64**	78.90	96.89
PA9	**85.64**	78.94	95.52
PA10	**82.00**	75.15	95.03
PA11	**79.90**	76.29	86.69

In addition, It was analyzed by calculating the Accuracy of SUV of MATLAB scheme and Xeleris workstation, then the comparison of them were performed. From the table above show the mean of accuracy is 85.47%.

SUV results from both systems in each individual patient agreed favorably. The SUV from Xeleris workstation gives high value than the SUV from MATLAB scheme for all readings.

CHAPTER VI
DISCUSSION

The accuracy of estimate is expressed by confident interval with specific confidence level. At 95% confident interval, the accuracy of SUV from the MATLAB scheme is 85%. Nonetheless, it gives a lower SUV compared to the Xeleris workstation in all study.

The related parameters which are used in this SUV calculation scheme are different in data type, so the conversion is mainly needed in every step. The result may possibly because of the data lost in conversion step.

Since defined the MATLAB scheme in term of the amount of SUV value, we found that the small value of SUV gives high accuracy compared to the large. It means that the MATLAB scheme is high effective for used with the small SUV.

After reviewing most of the related literatures, it was found that many freeware currently supported the PET DICOM file but it is usable only for image reviewing. The application software, which is provided the SUV calculation still negligibly launched.

The data viewing, analysis and interpretation in a PET / CT scanning are often done by software that installed within the workstation area or where the PACS is accessible. Besides, the application software is generally from the same manufacturer of the scanner. These are the problem and reason that is leading to this research.

The sample source of this research is DICOM files. These are archived from PET/CT Discovery STE (DSTE) scanner. In the comparative study, it was tested by comparing with the Xeleris workstation. Both DSTE and Xeleris workstation are manufactured by GE healthcare and routinely operated in Siriraj Imaging Center.

DICOM file is supported by MATLAB which the scientists widely used now a day. So, it is suitable for using as a tool for the data analysis.

So, from the performance test of the new scheme showed an agreeable result. These are practical to medical prognosis and research.

The accomplishment of the new scheme offers a great deal advantage. It provided simple and convenient in data accessibility.

CHAPTER VII
CONCLUSION

This research presented the SUV calculation in a new technique. The study was divided into 2 main sections. The first section is about the creation of SUV calculation scheme and the second section is about the scheme testing. However, for more understanding, the pilot study was done firstly.

The new technique is to create an application program for SUV calculation from PET/CT DICOM file. DICOM is a unique file type that contains both image and metadata. This scheme was written by using MATLAB. MATLAB was used for extracting and gathering data from DICOM.

In the section of the scheme testing, the performance was tested practically using the patient's scan. The scheme was compared to the well known application program from GE healthcare.

The results showed that the correlation between two systems were statistically significant with 99% confidence interval. The average of percentage accuracy was 85% and for the report at 95% confidence interval, ranged from 83.91% to 86.48%.

The agreeable results above were represented in order to reassure that the scheme of SUV calculation provided the correct SUV value. It can be interchangeably used for PET/CT analysis and interpretation instead of the application from any well-known vendor.

Generally, Vendor's DICOM is not always useable by another vendor's products. The application software is built up for using with its own scanner. That is a weakness of the application software in today's market. So the new scheme was created to eliminate that limitation.

In an ideal scheme, it should be able to read all every vendor's DICOM. But in this research DICOM files from PET/CT DISCOVERY STE (DSTE) were

used. It is a scanner of GE healthcare's vendor. DSTE is an only PET/CT scanner which is used in Siriraj Imaging Center.

The SUV scheme in this research was created by DICOM file based on the attribute of GE's vendor. Each vendor implements DICOM in its own dialect. Even though, the SUV calculation is based on the fundamental formula, but different vendor's DICOM impose slightly different method. So, this SUV scheme was supported only for GE's DICOM. However, it can be simply completed more ultimately in a future.

This scheme was created by using MATLAB language. MATLAB is a technical computing language which is a widely used tool in science and engineering community. It allows creation of user interfaces. Therefore, the scheme can be developed to be the convenient and easy-to-use application program with an uncomplicatedly approach. Moreover, instead of MATLAB, the scheme can also be written in any other programming language.

REFERENCES

1. Thie JA. Understanding the standardized uptake value, its methods, and implications for usage. J Nucl Med. 2004 Sep;45(9):1431-4.
2. Meirelles GS, Kijewski P, Akhurst T. Correlation of PET/CT standardized uptake value measurements between dedicated workstations and a PACS-integrated workstation system. J Digit Imaging. 2007 Sep;20(3):307-13.
3. Teras M, Tolvanen T, Johansson JJ, Williams JJ, Knuuti J. Performance of the new generation of whole-body PET/CT scanners: Discovery STE and Discovery VCT. Eur J Nucl Med Mol Imaging. 2007 Oct;34(10):1683-92.
4. Digital Imaging and Communication in Medicine (DICOM) Positron emission tomography image objects Supplement 12 ACR-NEMA
5. Technical Publication Advance TM 5.1 Conformance Statement for DICOM V3.0. In: System GM, editor.: General Electric Healthcare. p. 3_17-3_21.
6. Kanakatte A, Gubbi J, Mani N, Kron T, Binns D, editors. Pilot Study of Automatic Lung Tumor Segmentation from Positron Emission Tomography Images using Standard Uptake Values. Computational Intelligence in Image and Signal Processing, 2007 CIISP 2007 IEEE Symposium on 2007 1-5 April; Honolulu, HI IEEE.
7. Saha GB. Basics of PET imaging : physics, chemistry, and regulations. 2nd ed. New York ; London: Springer; 2010.
8. Bailey DL. Positron emission tomography : basic sciences. New York: Springer; 2005.
9. Jadvar H, Parker JA. Clinical PET and PET/CT. London: Springer; 2004.
10. Ollinger JM, Fessler JA. Positron-emission tomography. Signal Processing Magazine, IEEE. 1997;14(1):43-55.
11. Powsner RA, Powsner ER. Essential nuclear medicine physics. 2nd ed. Malden, Mass.: Blackwell Pub.; 2006.

12. Alessio A, Kinahan P. PET Image Reconstruction. In: Henkin RE, editor. Nuclear Medicine (2nd ed). 2nd ed. Philadelphia: Mosby Elsevier; 2006. p. 2 v. (xxvi, 1744 p., xliv).

13. Kapoor V, McCook BM, Torok FS. An introduction to PET-CT imaging. Radiographics. 2004 Mar-Apr;24(2):523-43.

14. Wang Y, Chiu E, Rosenberg J, Gambhir SS. Standardized uptake value atlas: characterization of physiological 2-deoxy-2-[18F]fluoro-D-glucose uptake in normal tissues. Mol Imaging Biol. 2007 Mar-Apr;9(2):83-90.

15. Soret M, Bacharach SL, Buvat I. Partial-volume effect in PET tumor imaging. J Nucl Med. 2007 Jun;48(6):932-45.

16. Boellaard R, Krak NC, Hoekstra OS, Lammertsma AA. Effects of noise, image resolution, and ROI definition on the accuracy of standard uptake values: a simulation study. J Nucl Med. 2004 Sep;45(9):1519-27.

17. Ivanovic M, McCartney WH, Amir Khandani, editors. Standard Uptake Value in Whole-Body FDG PET: Effects of Acquisition and Processing Parameters. Nuclear Science Symposium Conference Record; 2004 19-25 October; Rome: IEEE.

18. Ivanovic M, McCartney WH, Amir Khandani, editors. Evaluation of PET Standard Uptake Values Dependence on Imaging Protocal for Dual Time Point Imaging. Nuclear Science Symposium Conference Record; 2004 16-22 October; Rome: IEEE.

19. Beaulieu S, Kinahan P, Tseng J, Dunnwald LK, Schubert EK, Pham P, et al. SUV varies with time after injection in (18)F-FDG PET of breast cancer: characterization and method to adjust for time differences. J Nucl Med. 2003 Jul;44(7):1044-50.

20. Sajdak R, Halama J, Wagner R. Critical technical factors affecting the standardized uptake value (SUV) calculation for FDG PET. Society of Nuclear Medicine Annual Meeting Abstracts. 2006;47(suppl_1):531P-a.

21. ACRIN Qualification procedure for PET or PET/CT Imaging: American collage of radiology imaging network; 2007.

22. PET Phantom Instructions for Evaluation of PET Image Quality: American Collage of Radiology Imaging Network.

23. Zanzonico P. Routine quality control of clinical nuclear medicine instrumentation: a brief review. J Nucl Med. 2008 Jul;49(7):1114-31.

24. The Standardized Quality Control Procedures to Monitoring the PET scanner Performance Using Uniformity Phantoms : One-year Experiences and result.: 36th Annual Scientific Meeting of the Australian and New Zealand Society of Nuclear Medicine(2006).

25. A Retrospective Analysis of Accuracy and Reproducibility of SUV Determination Based on Phantom Experiments: 36th Annual Scientific Meeting of the Australian and New Zealand Society of Nuclear Medicine(2006).

26. J.Novoa F, F.Castro A, Pereira J, Pazos A, editors. Development of a DICOM server for the reception and storage of medical images in digital format. the 4th WSEAS International Conference on Applied Information and communication; 2004; Wisconsin, USA World Scientific and Engineering Academy and Society (WSEAS)

27. Soongsathitanon S. Wavelet-based Image Compression using a new patial search LBG Algorithm. 2007 [cited 6 5]; 715-21].

28. Soongsathitanon S, editor. A novel LBG algorithm for image compression in wavelet transform domain. the 11th WSEAS International Conference on Applied Mathematics,; 2007; Wisconsin, USA World Scientific and Engineering Academy and Society (WSEAS).

29. Jiménez-Herrera A, Avilés-Cruz C, Arechiga-Martínez R, editors. Minimum PACS system based on DICOM standard. The 11th WSEAS International Conference on Computers; 2007; Agios Nikolaos, Crete Island, Greece. 1353998: World Scientific and Engineering Academy and Society (WSEAS).

30. Doyle AJ, Le Fevre J, Anderson GD. Personal computer versus workstation display: observer performance in detection of wrist fractures on digital radiographs. Radiology. 2005 Dec;237(3):872-7.

31. McDonald L, Cramer B, Barrett B. Detection rates in pediatric diagnostic imaging: A picture archive and communication system compared with a web-based imaging system. Can Assoc Radiol J. 2006 Feb;57(1):30-4.

32. Lee W-J, Lee H-T, Ching Y-T, Tsai C-H, Liu H-M, Shyh-Jye Chen. Tablet PC as a PACS workstation : Observer Performance Evaluation. Chin Journal of Radiology. 2005;30:277-81.

33. Pianykh OS. Digital imaging and communications in medicine (DICOM) : a practical introduction and survival guide. Berlin: Springer; 2008.

34. Madsen MT. Selecting a new PET/CT system. J Am Coll Radiol. 2004 May;1(5):356-8.

35. DiscoverySTE Quick Manual. In: System GM, editor.: General Electric Healthcare p. 28-38.

36. Quantitative Imaging Biomarkers Alliance (QIBA). Available from: http://qibawiki.rsna.org/.

APPENDIX

PA 1

Sex : Female
Height :152 cm.
Weight : 52 kg

Position
Region A : X = 44.9 Y = 72.3

Activity	570 Mbq	at 8.57 a.m.
• **Administrated**	-	at 9.07 a.m
• **Scan**	351 Mbq	at 10.06 a.m.
• **Residual**	22.20 Mbq	at 8.57 a.m.

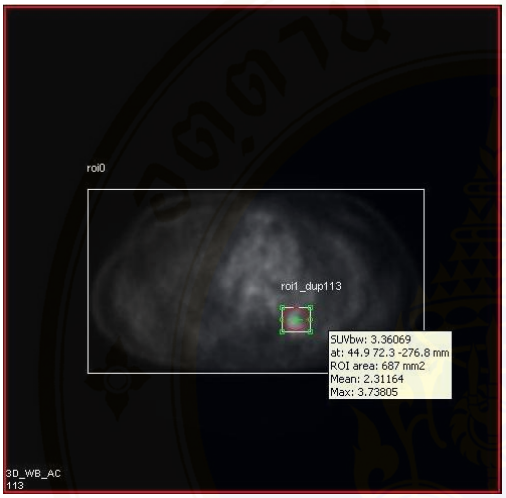

Slice No. on		SUV_{max}		% Accuracy
Xeleris	DICOM	**Xeleris**	**MATLAB**	
Region A				
113	187	3.3607	3.089	**91.92**
114	186	3.8359	3.529	**92.00**
115	185	4.1422	4.264	**97.06**
116	184	5.3920	4.904	**90.95**
117	183	6.5570	5.423	**82.71**
118	182	7.5530	6.241	**82.63**
119	181	7.4908	6.217	**83.00**
120	180	7.1687	5.923	**82.62**
122	178	4.7032	3.886	**82.62**
123	177	3.2456	2.682	**82.63**
mean		**5.34**	**4.62**	**86.79**

PA 2

Sex : Male
Height :cm.
Weight : kg

Activity		Mbq	at	a.m.
•	**Administrated**	-	at	a.m.
•	**Scan**	Mbq	at	a.m.
•	**Residual**	Mbq	ata.m.	

Position
Region A1 : X = 84.0Y = 21.5
Region B1 : X = -76.2Y = 33.2
Region A2 : X = 115.2 Y = 29.3
Region B2 : X = -107.4 Y = 21.5

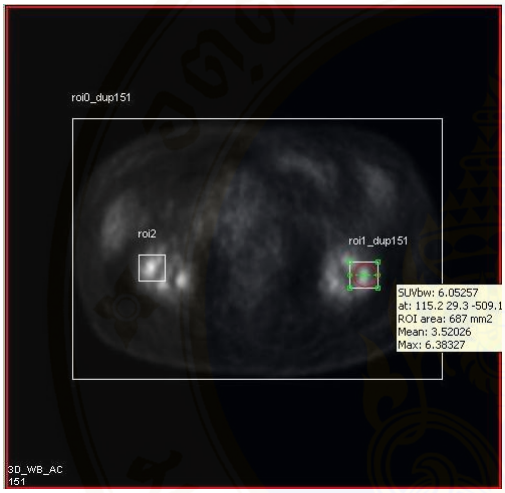

Slice No. on		SUV_{max}		% Accuracy
Xeleris	DICOM	**Xeleris**	**MATLAB**	
Region A2				
151	149	5.26	5.07	**96.39**
152	148	7.09	5.64	**79.55**
153	147	6.29	4.99	**79.33**
154	146	4.88	4.62	**94.67**
Region B2				
151	149	8.44	6.71	**79.50**
152	148	7.55	6.00	**79.47**
153	147	6.37	5.15	**80.85**
154	146	4.79	4.39	**91.65**
mean		**6.33**	**5.32**	**85.17**

PA 3

Sex : Female
Height : 146 cm.
Weight : 44 kg

Activity		566.099 Mbq	at 8.33a.m.
•	**Administrated**	-	at 8.37 a.m
•	**Scan**	359.5 Mbq	at 9.40 a.m.
•	**Residual**	16.31 Mbq	at8.38a.m.

Position
Region A1 : X = -41.0Y = 29.3
Region B1 : X = --41.0 Y = 21.5

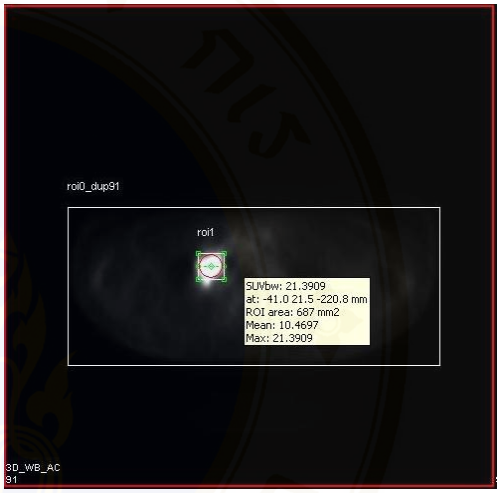

Slice No. on		SUV_{max}		% Accuracy
Xeleris	DICOM	**Xeleris**	**MATLAB**	
Region A				
83	181	10.17	8.51	**83.68**
84	180	16.83	13.68	**81.28**
85	179	21.77	17.70	**81.30**
86	178	24.10	19.59	**81.29**
87	177	22.08	18.36	**83.15**
88	176	18.40	16.48	**89.57**
89	175	16.50	16.68	**98.91**
90	174	15.87	15.47	**97.48**
Region B				
91	173	21.39	17.39	**81.30**
92	172	21.83	17.74	**81.26**
93	171	18.85	16.05	**85.15**
mean		**18.89**	**16.15**	**85.55**

PA 4

Sex : Male
Height : 170 cm.
Weight : 56 kg

Activity		349.279Mbq	at 9.00 a.m.
•	**Administrated**	-	at 9.03 a.m
•	**Scan**	222.3Mbq	at 10.00 a.m.
•	**Residual**	22.496Mbq	at 9.04 a.m.

Position
Region A1 : X = -41.0Y = 29.3
Region B1 : X = --41.0 Y = 21.5

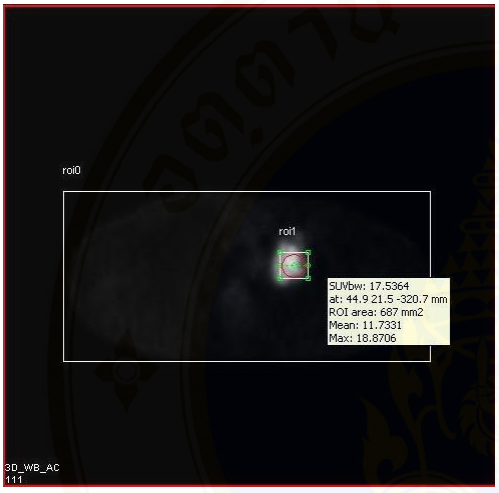

Slice No. on		SUV_{max}		% Accuracy
Xeleris	DICOM	**Xeleris**	**MATLAB**	
Region A				
111	225	17.54	15.84	**90.31**
112	224	18.14	15.86	**87.43**
113	223	15.94	16.55	**96.17**
114	222	14.13	16.29	**84.71**
Region B				
115	221	21.00	17.63	**83.95**
116	220	20.35	17.17	**84.37**
117	219	20.47	17.19	**83.98**
118	218	16.57	14.97	**90.34**
mean		18.02	16.44	**87.66**

PA 5

Sex : Male
Height : 170 cm.
Weight : 78 kg

Activity			
•	**Administrated**	-	at 8.53a.m
•	**Scan**	352.1Mbq	at 9.56 a.m.
•	**Residual**	22.53Mbq	at 8.55 a.m.

Position
Region A1 : X = 142.6 Y = 52.7
Region B1 : X = 134.8 Y = 64.5

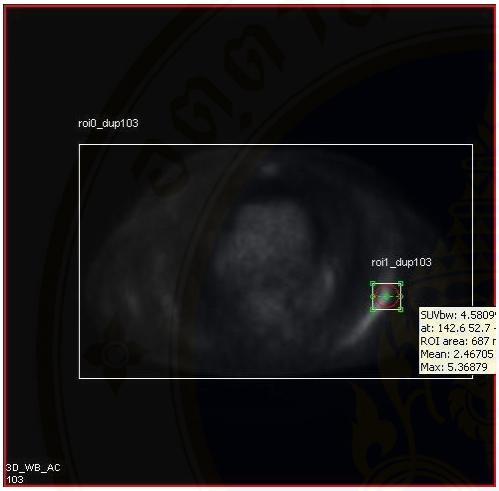

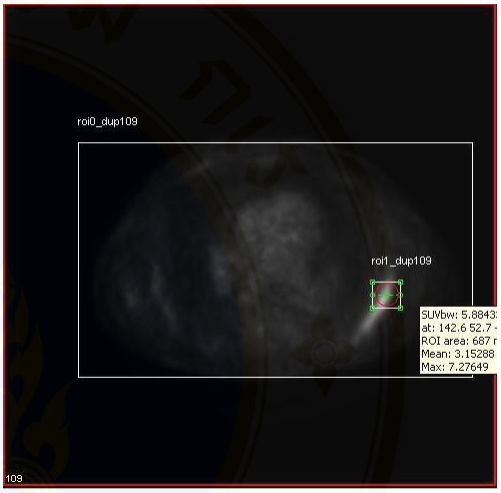

Slice No. on		SUV_{max}		% Accuracy
Xeleris	DICOM	**Xeleris**	**MATLAB**	
Region A				
103	197	4.58	4.34	**94.76**
104	196	6.25	5.06	**80.96**
105	195	7.02	5.67	**80.77**
106	194	8.19	6.63	**80.95**
107	193	7.01	6.36	**90.73**
108	192	7.04	6.52	**92.61**
Region B				
109	191	6.59	5.88	**89.23**
110	190	6.10	5.29	**86.72**
111	189	4.96	4.58	**92.34**
112	188	4.67	4.01	**85.87**
mean		6.24	5.43	**87.40**

PA 6

Sex : Male
Height : 165 cm.
Weight : 46 kg

Position
Region A1 : X = 33.2 Y = 2.0

Activity			
•	**Administrated**	-	at 9.16a.m
•	**Scan**	200.9 Mbq	at 10.13 a.m.
•	**Residual**	253.08Mbq	at 9.16 a.m.

Slice No. on		SUV_{max}		% Accuracy
Xeleris	DICOM	**Xeleris**	**MATLAB**	
Region A				
135	165	13.91	12.72	**91.45**
136	164	15.76	13.68	**86.80**
137	163	15.81	14.16	**89.56**
138	162	17.68	14.76	**83.48**
139	161	20.49	16.45	**80.28**
140	160	23.01	18.47	**80.27**
141	159	22.98	18.93	**82.38**
142	158	21.31	18.98	**89.07**
143	157	22.55	18.67	**82.79**
144	156	25.28	20.29	**80.26**
146	154	24.87	20.29	**81.58**
147	153	21.45	19.48	**90.82**
148	152	17.10	17.11	**99.94**
mean		20.17	17.23	**85.89**

PA 7

Sex : Male
Height : 180 cm.
Weight : 66 kg

Activity			
•	**Administrated**	-	at 8.29a.m
•	**Scan**	358.3Mbq	at 9.36 a.m.
•	**Residual**	22.05Mbq	at 8.31 a.m.

Position
Region A1 : X = -33.2 Y = 2.0

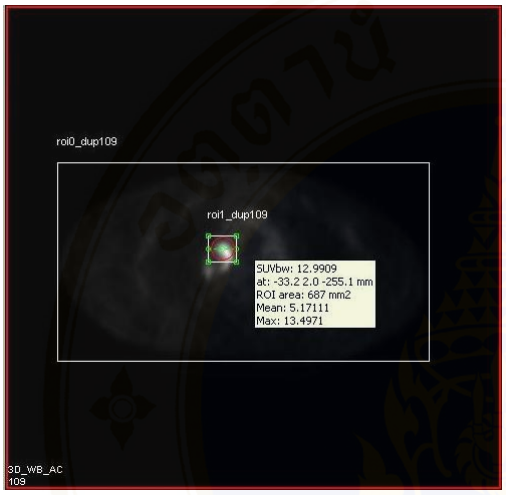

Slice No. on		SUV_{max}		% Accuracy
Xeleris	DICOM	**Xeleris**	**MATLAB**	
Region A				
109	227	12.99	10.66	**82.06**
110	226	13.23	10.45	**78.99**
111	225	12.76	10.08	**79.00**
112	224	13.18	10.41	**78.98**
113	223	12.24	9.66	**78.92**
114	222	9.32	7.60	**81.55**
115	221	5.97	5.90	**98.83**
116	220	5.94	6.10	**97.31**
117	219	7.45	6.54	**87.79**
118	218	7.79	6.61	**84.85**
119	217	8.80	7.79	**88.52**
120	216	7.92	7.80	**98.48**
mean		9.80	8.30	**89.53**

PA 8

Sex : Male
Height : 60.5 cm.
Weight : 57 kg

Position
Region A : X = 60.5 Y = 60.5
Region B : X = 48.8 Y = 56.6

Activity	400.709Mbq	at 8.53 a.m.
• **Administrated**	-	at 8.59 a.m
• **Scan**	246.8Mbq	at 10.06 a.m.
• **Residual**	7.362 Mbq	at 9.00 a.m.

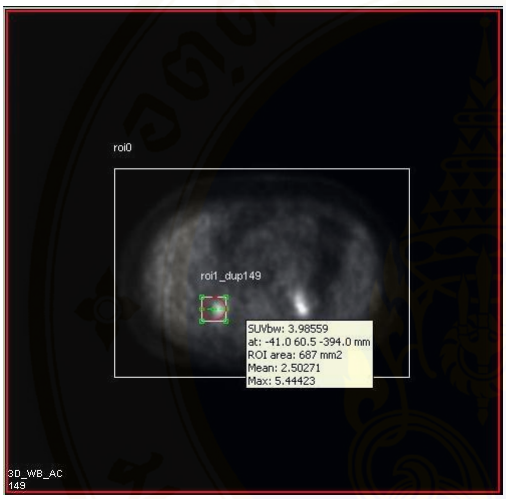

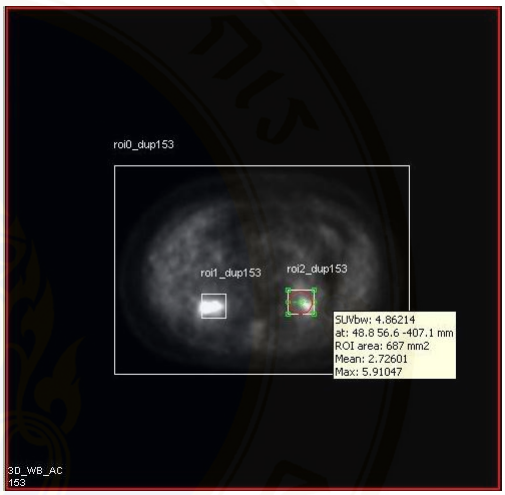

Slice No. on		SUV_{max}		% Accuracy
Xeleris	DICOM	**Xeleris**	**MATLAB**	
Region A				
149	151	3.99	4.30	**92.23**
150	150	7.44	6.93	**93.15**
151	149	10.17	8.70	**85.55**
152	148	12.15	9.60	**79.01**
Region B				
149	151	6.59	5.44	**82.55**
150	150	7.06	5.57	**78.90**
151	149	8.04	6.60	**82.09**
152	148	7.99	6.31	**78.97**
153	147	4.82	4.67	**96.89**
mean		7.58	6.46	**84.64**

PA 9

Sex : Male
Height : 184 cm.
Weight : 113 kg

Position
Region A : X = 52.7 Y = -25.4

Activity	640.099Mbq	at 8.35 a.m.
• **Administrated**	-	at 8.42a.m
• **Scan**	387.3 Mbq	at 9.47 a.m.
• **Residual**	25.71 Mbq	at 8.42 a.m.

Slice No. on		SUV_{max}		% Accuracy
Xeleris	DICOM	**Xeleris**	**MATLAB**	
Region A				
81	219	9.38	9.80	**95.52**
82	218	16.59	13.24	**79.81**
83	217	20.07	16.02	**79.82**
84	216	16.42	15.52	**94.52**
85	215	10.98	12.91	**82.42**
86	214	10.21	12.36	**78.94**
87	213	12.88	13.94	**91.77**
88	212	12.08	14.22	**82.28**
mean		13.58	13.50	**85.64**

PA 10

Sex : Male
Height : 163 cm.
Weight : 34 kg

Activity		481.369Mbq	at 8.45 a.m.
•	**Administrated**	-	at8.49 a.m
•	**Scan**	286.2Mbq	at 10.04 a.m.
•	**Residual**	8.029Mbq	at 8.52 a.m.

Position
Region A : X = -56.6 Y = 13.7
Region B : X = -154.3 Y = -72.3

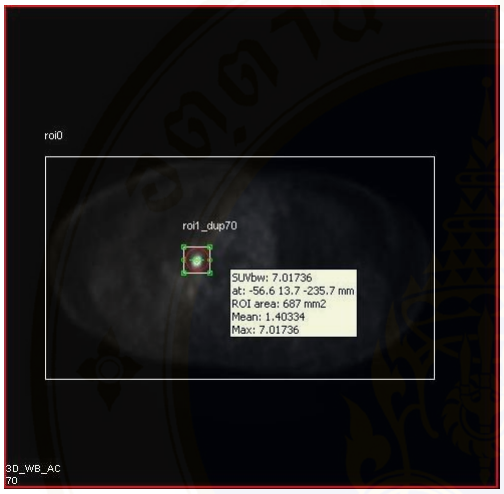

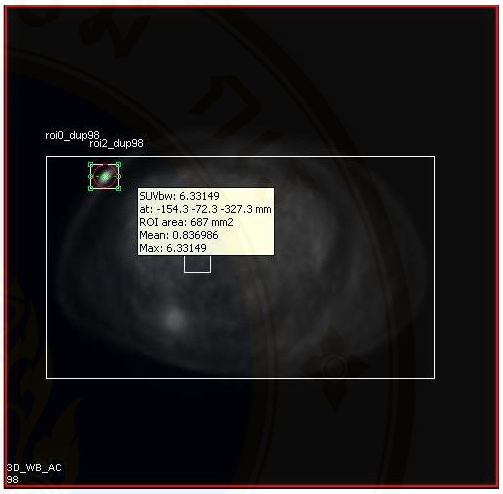

Slice No. on		SUV_{max}		% Accuracy
Xeleris	DICOM	**Xeleris**	**MATLAB**	
Region A				
71	229	12.42	9.34	**75.20**
72	228	14.89	11.19	**75.15**
73	227	13.08	13.73	**95.03**
74	226	9.85	9.30	**94.42**
75	225	4.07	3.69	**90.66**
Region B				
98	202	6.33	4.76	**75.20**
99	201	27.22	20.46	**75.17**
100	200	48.12	36.18	**75.19**
101	199	29.59	22.25	**75.19**
102	198	5.64	4.24	**75.18**
mean		17.13	13.51	**82.00**

PA 11

Sex : Male
Height : 155 cm.
Weight : 58 kg

Position
Region A : X = -48.8 Y = 13.7
Region B : X = -68.4 Y = 25.4

Activity	566.099 Mbq	at 8.33 a.m.
• **Administrated**	-	at 8.37 a.m
• **Scan**	359.5 Mbq	at 9.40 a.m.
• **Residual**	16.31 Mbq	at 8.38 a.m.

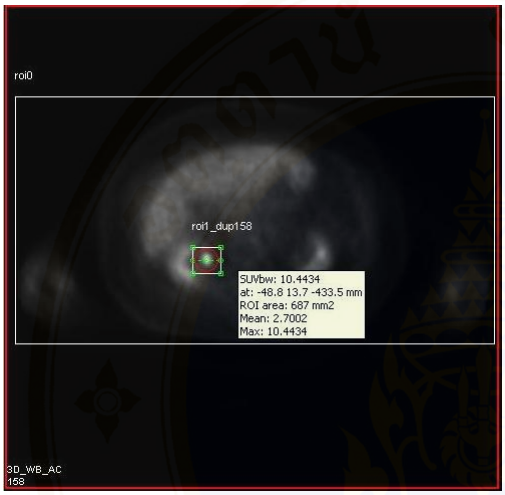

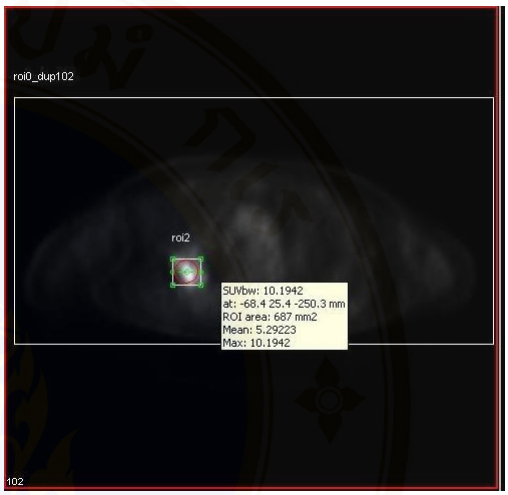

Slice No. on		SUV_{max}		% Accuracy
Xeleris	DICOM	**Xeleris**	**MATLAB**	
Region A				
158	142	10.44	7.97	**76.34**
159	141	17.22	13.14	**76.31**
160	140	19.10	14.58	**76.34**
161	139	10.29	7.85	**76.29**
Region B				
101	199	7.62	6.38	**83.73**
102	198	10.19	7.78	**76.35**
103	197	7.02	8.11	**84.47**
104	196	9.39	8.14	**86.69**
105	195	6.29	7.61	**79.01**
mean		10.84	9.06	**79.90**

ALL PATIENTS

The SUV rearranged by sorting the smallest to the largest.

- SUV<5

	Xeleris	MATLAB	%Accuracy
1	2.11	1.83	86.54
2	3.25	2.68	82.64
3	3.36	3.09	91.92
4	3.84	3.53	92.00
5	3.99	4.30	92.11
6	4.07	3.69	90.48
7	4.14	4.26	97.06
8	4.58	4.34	94.78
9	4.67	4.01	85.94
10	4.70	3.89	82.62
11	4.79	4.39	91.56
12	4.82	4.67	96.82
13	4.88	4.62	94.64
14	4.96	4.58	92.35

- 5<SUV<10

	Xeleris	MATLAB	%Accuracy
15	5.26	5.07	96.46
16	5.39	4.90	90.95
17	5.64	4.24	75.18
18	5.94	6.10	97.37
19	5.97	5.90	98.86
20	6.10	5.29	86.70
21	6.25	5.06	80.86
22	6.29	4.99	79.46
23	6.29	7.61	79.01
24	6.33	4.76	75.18
25	6.37	5.15	80.90
26	6.56	5.42	82.71
27	6.59	5.44	82.55
28	6.59	5.88	89.25
29	7.01	6.36	90.78
30	7.02	5.67	80.87
31	7.02	5.28	75.18
32	7.04	6.52	92.52
33	7.06	5.57	78.98
34	7.09	5.64	79.45
35	7.17	5.92	82.62
36	7.44	6.93	93.11
37	7.45	6.54	87.74
38	7.49	6.22	83.00
39	7.55	6.00	79.45
40	7.55	6.24	82.63
41	7.62	6.38	83.74
42	7.79	6.61	84.79
43	7.92	7.80	98.49
44	7.99	6.31	78.99
45	8.04	6.60	82.18
46	8.19	6.63	80.87
47	8.44	6.71	79.45
48	8.80	7.79	88.49
49	9.32	7.60	81.57
50	9.38	9.80	95.62
51	9.39	8.14	86.71
52	9.85	9.30	94.35

- 10<SUV<15

	Xeleris	MATLAB	%Accuracy
53	10.17	8.70	85.50
54	10.17	8.51	83.68
55	10.19	7.78	76.30
56	10.21	12.36	78.95
57	10.29	7.85	76.32
58	10.44	7.97	76.31
59	10.98	12.91	82.40
60	12.08	14.22	82.24
61	12.15	9.60	78.98
62	12.24	9.66	78.97
63	12.42	9.34	75.19
64	12.76	10.08	79.00
65	12.88	13.94	91.73
66	12.99	10.66	82.06
67	13.08	13.73	95.03
68	13.18	10.41	78.98
69	13.23	10.45	78.99
70	13.91	12.72	91.47
71	14.13	16.29	84.69
72	14.89	11.19	75.16

- 15<SUV<20

	Xeleris	MATLAB	%Accuracy
73	15.76	13.68	86.82
74	15.81	14.16	89.58
75	15.87	15.47	97.46
76	15.94	16.55	96.15
77	16.42	15.52	94.54
78	16.50	16.68	98.91
79	16.57	14.97	90.33
80	16.59	13.24	79.80
81	16.83	13.68	81.30
82	17.10	17.11	99.96
83	17.22	13.14	76.31
84	17.54	15.84	90.33
85	17.68	14.76	83.46
86	18.14	15.86	87.42
87	18.40	16.48	89.58
88	18.85	16.05	85.14
89	19.10	14.58	76.32

- SUV>20

	Xeleris	MATLAB	%Accuracy
90	20.07	16.02	79.80
91	20.35	17.17	84.38
92	20.47	17.19	83.97
93	20.49	16.45	80.28
94	21.00	17.63	83.96
95	21.31	18.98	89.06
96	21.39	17.39	81.30
97	21.45	19.48	90.84
98	21.77	17.70	81.29
99	21.83	17.74	81.27
100	22.08	18.36	83.16
101	22.55	18.67	82.78
102	22.98	18.93	82.38
103	23.01	18.47	80.27
104	24.10	19.59	81.28
105	24.87	20.29	81.57
106	25.28	20.29	80.25
107	27.22	20.46	75.17
108	29.59	22.25	75.20

BIOGRAPHY

NAME Miss Pawitra Masa-ah

DATE OF BIRTH 17 May 1983

PLACE OF BIRTH Narathiwat, Thailand

INSTITUTIONS ATTENDED Thaksin University, Songkhla 2000-2004
Bachelor of Science (Physics)
Mahidol University, 2007-2011
Master of Science (Radiological Science)

HOME ADDRESS 131 M.6, Saithong1 road,
Pasaymas, Sungaikolok
Narathiwat
Tel. 073-614312
E-mail : wana_pawitra@hotmail.com

PUBLICATION

1. Masa-Ah P, Soongsathitanon S. A Novel Standardized Uptake Value (SUV) Calculation of PET DICOM Files Using MATLAB. In: Mastorakis PNE, Mladenov PV, Bojkovic PZ, editors. NEW ASPECTS of APPLIED INFORMATICS, BIOMEDICAL ELECTRONICS & INFORMATICS and COMMUNICATIONS: WSEAS Press; 2010. p. 413-6.

2. Masa-Ah P, Tuntawiroon M, Soongsathitanon S. A Novel Scheme for Standardized Uptake Value (SUV) Calculation in PET Scans. INTERNATIONAL JOURNAL OF MATHEMATICAL MODELS AND METHODS IN APPLIED SCIENCES, NAUN. 2010; 4(4):291-9.

PRESENTATION

A Novel Standardized Uptake Value (SUV) Calculation of PET DICOM Files Using MATLAB: 3rd WSEAS International Conference on BIOMEDICAL ELECTRONICS and BIOMEDICAL INFORMATICS (BEBI '10) (August 20-22, 2010) Taipei, Taiwan World Scientific and Engineering Academy and Society (WSEAS).